4-29-2002

# A novel membrane process for autotrophic denitrification

Agnieszka Pierkiel
*Rowan University*

# A NOVEL MEMBRANE PROCESS FOR AUTOTROPHIC DENITRIFICATION

by
Agnieszka Pierkiel

A Thesis

Submitted in partial fulfillment of the requirements of the
Master of Science Degree
of
The Graduate School
at
Rowan University
May, 2002

Approved by _____

Date Approved April 29, 2002

# ABSTRACT

Agnieszka Pierkiel, A Novel Membrane Process for Autotrophic Denitrification, 2002, Kauser Jahan. Ph.D.,P.E., Environmental Engineering.

This research focused on the novel use of hollow fiber membranes for gas delivery in biological dentrification using hydrogen-oxidizing bacteria. Autotrophic denitrification is a biological process that reduces nitrate to nitrogen gas using an inorganic carbon source. Hydrogen gas is an electron donor and nitrate is the electron acceptor in the reaction. The specific research objectives were to:

- *develop* a mixed acclimated culture of hydrogen-oxidizing bacteria;
- *evaluate* biodegradation kinetics of the acclimated culture;
- *evaluate* hydrogen transfer characteristics of hollow fiber membrane modules; and
- *demonstrate* technical feasibility of a continuous bioreactor-membrane system for denitrification.

The following kinetic coefficients were obtained: $\mu_m$ of 0.65 $d^{-1}$, Y of 0.78 mg cells/mg $NO_3$-N, and $k_d$ of 0.04 $d^{-1}$. The nitrate utilization rate was determined to be 1.0 mg $NO_3$-N/mg biomass. The following mass transfer correlation can be used to design membrane modules for hydrogen dissolution into water:

$$Sh = 2.68\ Red_e/L^{1.02}Sc^{0.33}$$

Continuous flow studies indicate that a stable biofilm can be developed in a packed bed reactor to remove nitrate using hydrogen as the electron donor. Hydrogen gas was successfully delivered to the reactor via the hollow fiber membrane gas transfer module without fouling. Dissolved hydrogen concentrations indicate that the system did not experience hydrogen limitations. Membrane gas delivery appears to be a viable technology for transferring hydrogen to water for autotrophic denitrificiation.

# MINI-ABSTRACT

Agnieszka Pierkiel, A Novel Membrane Process for Autotrophic Denitrification, 2002, Kauser Jahan. Ph.D.,P.E., Environmental Engineering.

The purpose of this study was to determine the technical feasibility of a novel membrane technology for hydrogenotrophic denitrification of water. Biological kinetics were evaluated. A mass transfer correlation was developed for hollow fiber contactors for hydrogen delivery. Biological denitrification was successfully accomplished in a fixed bed bioreactor membrane system.

# ACKNOWLEDGEMENTS

I would like to thank my advisor, Dr. Kauser Jahan, for giving me an opportunity to work with her and for the encouragement and support during the course of my research. I would also like to thank my committee members Dr. Kathryn Hollar and Dr. C. Stewart Slater for their valuable suggestions and review of this thesis.

I would like to acknowledge the Water Environment Research Foundation staff Amit Pramanik, Ph.D., Mary Strawn, and Charles Noss, Sc.D. and the research council liaison Dr. Bruce E. Rittmann.

Dr. Tariq Ahmed of TAMS Consultants deserves special recognition for the outstanding support of the project.

Thanks to a member of my project team Claire Steager for her friendship and assistance. I am very grateful to Marvin Harris for technical support of the laboratory experiments. I would also like to mention Margaret Jaques, Shira Perlis, and Marcus Roorda for all their help.

In a special way, I would like to thank my parents Halina and Roman J. Pierkiel. This would not have been possible without their encouragement and moral support.

This research would not have been possible without the financial support from the Water Environment Research Foundation (Grant No. 00-CTS-14ET) and Rowan University.

# TABLE OF CONTENTS

# LIST OF FIGURES

# LIST OF TABLES

# CHAPTER 1

# INTRODUCTION

## 1.1 Background

### 1.1.1 Nitrate in the Environment

Nitrate is one of the most common groundwater contaminants in the United States and elsewhere (Korom, 1992; Freeze and Cherry, 1979; Gayle et al., 1989; Kapoor and Viraraghavan, 1997). It is a thermodynamically stable and highly soluble nitrogen species, which is easily transported and accumulated in groundwater systems. These properties coupled with increased anthropogenic releases of nitrogen containing compounds have resulted in elevated nitrate concentrations in United States and European ground and surface waters.

Nitrate contamination originates from point and non-point sources. The majority of point source contributions are attributed to domestic and industrial wastewater discharges. Contamination of drinking water sources with nitrate may result from both human and animal waste disposal and discharge of the waste water from food processing, explosives manufacturing, $NO_x$ absorption in air stripping and recovery of nuclear fuels (Pekdemir *et al.*, 1998). Non-point sources have a larger impact and are associated with agricultural practices, fisheries, poultry operations, livestock feeding and residential septic tank effluents (Hallberg, 1989). A large number of drinking water

aquifers have nitrate concentrations approaching or already above the maximum contaminant level (MCL) of 10 mg/L $NO_3^-$-N established by the US Environmental Protection Agency (EPA, 1993). An investigation conducted by the US Geological Survey (AWWA, 1995) analyzed nutrient concentrations of 12,000 groundwater and 22,000 surface water samples between 1970 and 1992. The results of the survey indicated that nitrate levels in 20 percent of shallow private wells in US farming areas violate the federal drinking water standard and that 1 percent of public water supply wells exceed the limit. Surface waters down gradient of agricultural areas had elevated nitrate concentrations, but rarely exceeded the limit. Of the 3,351 private wells surveyed 9 percent had nitrate concentrations exceeding the 10 mg/L standard.

### 1. 1.2 Health and Environmental Consequences

There is a number of health and environmental consequences associated with nitrate contamination. Incidence of methemoglobinemia is related to ingestion of nitrate-contaminated water (Shuvai and Gruener, 1977). Methemoglobinemia or "blue baby syndrome" occurs in infants under six months and is life threatening without immediate medical attention. N-nitroso compounds are also formed from nitrates and are known to be carcinogenic. Nitrites are intermediates in nitrate biodegradation and are toxic to aquatic organisms (Metcalf and Eddy, 1991). Nitrate disposal in aquatic systems also accelerates the onset of eutrophication, a process in which the water becomes organically enriched leading to domination by aquatic weeds, transformation to marshland and eventulally to dry land (Metcalf and Eddy, 1991).

Health problems related to consumption of nitrate-contaminated drinking water have led to regulation by US Environmental Protection Agency (USEPA). The nitrate concentration standards (MCL's) in drinking water allow a limit content of less than 10ppm $NO_3$-N/l and 1ppm $NO_2$-N/l in drinking water (2001). The European standards are stricter, allowing a concentration of no more than 0.03 ppm $NO_2$-N /l (Urbain *et al.*, 1996). A recommended level for nitrate is 5.6 ppm NO3-N/l for the European Community (Kapoor and Viraraghvan, 1997). To comply with these standards, municipal water suppliers are faced with the need for efficient and cost effective nitrate removal processes.

### 1.1.3 Nitrate Removal

Nitrate removal or "denitrification" is usually accomplished through physicochemical or biological processes. There are a number of methods available for removing nitrate from water and wastewater (Weber and DeGiano, 1996; Eckenfelder, 1989). Separation methods used in denitrification include ion exchange (IX), reverse osmosis (RO), activated-carbon adsorption, and electrodialysis (ED). Advantages of these processes include immediate nitrate removal at process startup, simple process control, reliability and ease of monitoring.

In water treatment, ion exchange is currently the predominant method for removing nitrate in the United States. Even with the recent development of nitrate selective resins, the maintenance and operating costs are still high, and the production of concentrated waste brines create additional disposal problems. The biological

denitrification of spent ion exchange regenerant is an effective alternative to continuous disposal (Viraraghavan and Rao, 1990; van der Hoek et al., 1988; Clifford and Liu, 1993). The long-term operational problem with an IX/denitrification process is that anion exchange resins are susceptible to significant organic fouling.

In European countries, biological denitrification of drinking water using heterotrophic microorganisms held in fixed bed reactors (Delanghe *et al.*, 1994a and b; Lazarova *et al.*, 1992) is more common. These systems typically use methanol, ethanol or acetic acid as the organic carbon source. The residual organics, if not removed effectively, can increase the chlorine demand of the water or react with chlorine and form carcinogenic disinfection byproducts (DBPs). The unconsumed organic matter will contribute to the biological instability of the drinking water (Rittmann and Huck, 1989). The adverse effects associated with biological instability in the distribution system are: (a) increased microbial growth, (b) production of taste and odor generating compounds and (c) increased corrosion of pipes (Rittmann and Snoeyink, 1984). These effects have limited heterotrophic denitrification to wastewater applications in the United States, because chlorine is the predominant means for disinfection of potable water. In Europe, disinfection of drinking water is being accomplished by ozone or ultraviolet (UV) radiation.

### 1.1.4 Heterotrophic Denitrification

Biological denitrification is a process that uses microorganisms to convert nitrate to nitrogen gas. Bacteria use nitrate as the terminal electron acceptor in their respiratory

processes when oxygen concentrations are low. Denitrification consists of a sequence of enzymatic reactions leading to the evolution of nitrogen gas. The process may involve the formation of the following intermediates (Szekers *et al.* , 2001):

$$NO_3^- \rightarrow NO_2^- \rightarrow NO \rightarrow N_2O \rightarrow N_2 \qquad (1.1)$$

Biological dentrification can be heterotrophic or autotrophic. Heterotrophic denitrification is the most common method of removing nitrogen from municipal and industrial wastewaters (Metcalf and Eddy, 1991). The denitrification reactors follow nitrification processes that convert organic nitrogen and ammonia to nitrate. The denitrification reactors can be either suspended growth or attached growth with the latter being favored because it minimizes the space required. The disadvantages of heterotrophic denitrification are the costs incurred for adding an external organic carbon source for cell synthesis and the post-treatment needed to remove the residual organic contaminants (precursors of DBPs) and biomass before disinfection and final discharge.

### 1. 1.5 Autotrophic Denitrification

For autotrophic organisms no organic carbon source is required, rather carbon dioxide or bicarbonate is used for cell synthesis (Brezonik, 1977). For the energy source, autotrophic organisms require hydrogen or reduced-sulfur compounds. There are four groups of autotrophic denitrifiers (Mateju *et al.*, 1992): hydrogen- oxidizing bacteria, reduced sulfur oxidizing bacteria, ferrous oxidation bacteria, and chloric compound oxidizing bacteria. Hydrogen-oxidizing bacteria metabolize nitrates and

nitrites using hydrogen as an energy source and carbon dioxide or carbonate as the carbon source. In this reaction, nitrate or nitrite is the electron acceptor and hydrogen is the electron donor. Autotrophic denitrification with hydrogen-oxidizing bacteria is preferred for drinking water treatment because: (1) the residual hydrogen that remains in water is harmless and does not interfere with subsequent water treatment (Rittmann and Huck, 1989); (2) only inorganic carbon is used and therefore there are no organic residues for further treatment; and (3) reaction byproducts are harmless.

Autotrophic organisms, e.g., *Micrococcus denitrificans*, reduce nitrate to nitrite and subsequently to nitrogen gas while oxidizing hydrogen gas to water. The reaction proceeds as follows (Kurt *et al.*, 1987):

$$2NO_3^- + 2H_2 \rightarrow 2NO_2^- + 2H_2O \qquad (1.2)$$

$$2NO_2^- + 3H_2 \rightarrow N_2 + 2H_2O + 2OH^- \qquad (1.3)$$

Combining reactions 1.1 and 1.2 the overall reaction can be written as:

$$2NO_3^- + 5H_2 \rightarrow N_2 + 4H_2O + 2OH^- \qquad (1.4)$$

From the overall reaction given above, 2 moles of $OH^-$ are produced for every 2 moles of $NO_3^-$ reduced, so alkaline conditions (high pH) and $NO_2^-$ accumulation can be expected. To prevent pH shifts and nitrite accumulation, $CO_2$ or $HCO_3^-$ can be added to buffer the system as well as serve as the inorganic carbon source for cell synthesis. From the above equation, theoretically 0.35 mg $H_2$/mg $NO_3^-$-N is required for complete reduction of nitrate to nitrogen gas. The experimental values are: 0.38 mg $H_2$/mg $NO_3^-$-N in a

bench-scale fixed biofilm reactor (Kurt *et al.*, 1987) and 0.40 mg $H_2$/mg $NO_3^-$-N at a full-scale plant in Germany (Gross *et. al.*, 1986).

## 1.2 Denitrification Costs

The treatment costs of 100 lb of $NO_3^-$-N for hydrogen, methanol, ethanol and acetic acid are shown in Figure 1.1. The electron donor costs were calculated from a stoichiometric requirement. Current costs of chemicals were used for calculations. The cost analysis assumed no transportation costs for hydrogen, methanol, ethanol and acetic acid. The cost of hydrogen was found to lay within the range of organic electron donors ($11-$188). Methanol costs are 85% lower than hydrogen based on bulk chemical cost. However, if hydrogen were generated on site, the operating cost would decrease considerably. Ganzer (1995) reported cost of methanol to be about 73% greater than the cost associated with hydrogen use when generated on site. The transportation cost may be as high as the cost of the chemical itself depending on the actual location of the site. Therefore, if the transportation costs are included in the analysis, the use of hydrogen will be more economical.

The capital and operating cost for denitrification using an autotrophic process was also found to be higher than the cost of using heterotrophic denitrification (Mateju et al., 1992). However, the investigators assumed conventional bubble aeration system for dissolving hydrogen in water. The oxygen transfer efficiency (OTE) of such systems for oxygen is about 8-20% (WPCF, 1988). If the substrate is delivered in a stoichiometric quantity, the cost estimates of hydrogen and methanol change.

## 1.3 Research Goals and Objectives

The main goal of this study is to examine the technical feasibility of autotrophic denitrification of water and wastewater using membrane gas delivery to a fixed bed bioreactor. The specific objectives were to:

- *evaluate* batch biodegradation kinetics of the autotrophic denitrification process;
- *evaluate* the hydrogen gas transfer characteristics of hollow fiber membrane modules; and
- *develop* design procedures for continuous flow autotrophic attached growth fixed bed (plastic media) reactors coupled with membrane modules.

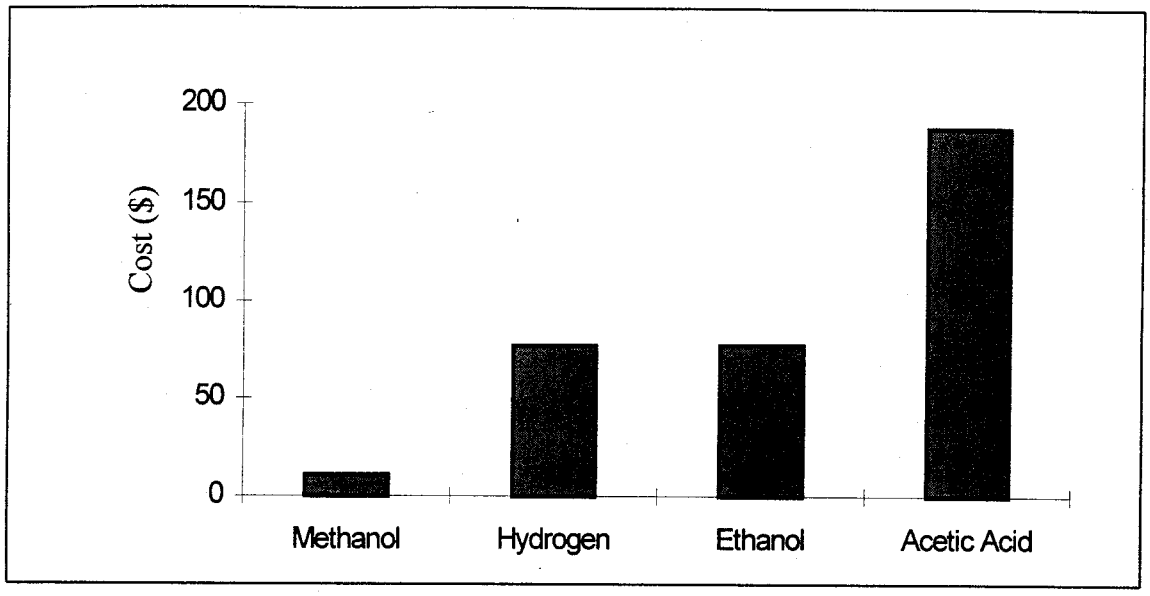


**Figure 1.1: Electron donor costs for biological denitrification of 100 lb $NO_3$-N**

# CHAPTER 2

# LITERATURE REVIEW

## 2.1 Introduction

Autotrophic denitrification is a relatively new research area. Interest in the process originated in Europe in the 1980's. Traditionally, European countries have been on the forefront of biological processes for drinking water treatment while the United States has focused on chemical and physical contaminant removal. Autotrophic denitrification has also increased in popularity in the Pacific Rim, including Japan and Taiwan. However, because of operational concerns including the hydrogen safety issue, there have been few actual hydrogen utilizing installations. Most recently, the technology has met with renewed interest due in part to novel developments in membrane research and technology which attempt to address these operating concerns.

A thorough literature review focusing on nitrate removal with hydrogen oxidizing bacteria is provided below. In this review, the following topics are discussed:

- autotrophic denitrification in fixed biofilm reactors,
- single-stage denitrification in fixed biofilm reactors,
- membrane applications in autotrophic denitrification, and
- modeling of biological kinetics.

Current research needs are summarized in the conclusion of the chapter.

## 2.2 Autotrophic Denitrification in Fixed Biofilm Reactors

Kurt et al. (1987) conducted extensive studies using autotrophic hydrogen-oxidizing denitrifying bacteria in a bench-scale fluidized bed reactor. Nitrite tended to accumulate in batch tests, but complete denitrification occurred in continuous flow experiments with sufficiently long residence times. A residence time of 4.5 hours was required for complete denitrification of water containing 25 mg/L $NO_3^-$–N. The optimum pH was found to be approximately 7.5, and the pH increased under unbuffered conditions. If the pH was allowed to rise near 9.0, nitrite tended to accumulate.

Gross et al. (1986) and Gross and Treutler (1986) reported on the start-up and performance of a commercial-scale biological-denitrification plant utilizing hydrogen. The technology was developed by Sulzer Water and Wastewater Treatment with the trade name DENITROPUR. The plant reached full capacity of 50 $m^3/h$ in approximately three months. The plant design incorporated indirect hydrogen saturation, phosphate addition, four packed-bed reactors in series, post-aeration, flocculant addition, filtration, and UV disinfection. Carbon dioxide was added as an inorganic carbon source and to buffer against an alkaline pH shift. At the operating temperature of 10.5°C, the organism growth rate varied from 0.1 to 0.3 $d^{-1}$. The sludge production was reported to be approximately 0.2 kg per kg nitrogen removed, on a dry-weight basis. Residence times of 1 to 2 hours were required to remove 50 mg/L nitrate.

Benedict *et al.* (1998) investigated the effect of reactor packing media on autotrophic denitrification with hydrogen oxidizing bacteria. Hydrogen and carbon dioxide were sparged into the feed water. The bench top biofilm reactors were packed with granular activated carbon, sand, pumice, volcanic rock, and polymer rings. A mixed

culture was obtained from a heterotrophic denitrification process in a water treatment facility. Nitrate and nitrite reduction was monitored daily at different hydraulic retention times. The highest removal efficiency with respect to surface area (770.4 mg $NO_3$-N/day) was achieved in the polymer ring bioreactor with an 8 hour hydraulic retention time. The performance of the polymeric rings medium was found to be superior to other investigated media in the range of 2 to 8 hours retention times. Nitrate reduction decreased with decreasing hydraulic retention time.

Long-term performance of an autotrophic denitrification process was evaluated by Szekers *et al.* (2001). The process was comprised of two steps: (1) the water to be treated was enriched with hydrogen in the cathodic chamber of an electrochemical cell and (2) denitrified in a fixed bed biofilm reactor. In the electrochemical cell, Nafion 417 cation-exchange membrane separated the two electrodes. Water was split by electrolysis into diatomic hydrogen and $OH^-$ ions at the cathode. The feed solution consisted of tap water with nitrate, carbonate, and phosphorus. It was hydrogenated in the cathodic chamber. As a result of the net reaction of denitrification, cathodic and anodic reaction, one mole of protons passed through the cation exchange membrane for each mole of nitrate.

The reactor was a packed bed of granulated activated carbon in an upflow configuration. The bioreactor was inoculated with a mixture of four denitrifying strains isolated from a previous reactor. The original inoculum was an enrichment culture from sediment from an oxidation pond treating domestic wastewater. The system was operated in a continuous mode for a period of one year. The feed concentration was kept constant at 21 mgN/L and water velocities ranged from 0.04 m/h to 0.2 m/h with current

densities from 40mA to 100mA. The rates of denitrification increased with water velocity at constant current of 80 mA until it reached 0.15 m/h when approximately 0.23 kg $N/m^3$day were removed with an effluent nitrite concentration below 1 mg N/L. The peak nitrate removal rate of 0.19 $kgN/m^3$day occurred at 70 mA in the runs at constant water velocity of 0.11 m/h. Denitrification rates up to 0.25 $kg\text{-}N/m^3$day were obtained at the hydraulic residence time of 1 h.

## 2.3 Single-stage Denitrification in Fixed Bed Reactors

Electrochemical applications have found their use in single-step denitrification. Electrodes were embedded in laboratory-scale sandy aquifers and hydrogen gas was produced through the electrolysis of water for enhancing autotrophic denitrification (Sakakibara and Kusaka, 1999). Groundwater containing 20 mg N/L of $NaNO_3$ and no electron donor was fed continuously to the synthetic aquifer. Denitrification rate varied depending on applied current. Electrical power requirement was 0.03-0.09 kWh/g N. Results showed that, when carbon electrodes were embedded in a direction perpendicular to groundwater flow, complete and stable denitrification was achieved over 1 year.

Immobilized systems can also be used for autotrophic denitrification in column configurations. *Ralstonia eutropha (Alcaligenes eutrophus)*, a hydrogen oxidizing bacteria, was immobilized in polyacrylamide and alginate copolymer beads which were then used as media in a fluidized bed reactor (Chang, 1999). The total reactor volume was 1L and 20% of the reactor volume was occupied by the immobilized beads. The reactor operated in continuous and batch mode. Feed contained nitrate and bicarbonate in deionized water and the hydraulic retention time was 400 min. The total nitrogen removal

rate in a continuous test increased with operation time and reached a maximum rate of 0.6-0.7 kg-N/$m^3$/day after 6 days. Nitrite reductase was inhibited when the dissolved hydrogen concentration fell below 0.2 mg/L, while nitrate reductase was inhibited at a concentration below 0.1 mg/L. A feed containing nitrate, bicarbonate, and phosphate in tap water was also investigated. Phosphate concentration affected denitrification especially in the accumulation of nitrite: as the concentration of phosphate increased, the accumulation of nitrite decreased. The bacteria were found to adapt to a shock nitrate loading.

Dries *et al.* (1988) tested a two-column system with removal of nitrate in the first column using polyurethane as support medium, and removal of excess hydrogen and oxidation of residual nitrite to nitrate in the second column. Water flowed downward in the denitrification column while hydrogen entered from the bottom. The water then passed through the second column in an upflow mode. Denitrification rates of 0.5 kg N/$m^3$day were obtained at 20°C. Although one full-scale system is being used in Europe, the process did not receive much attention because of the following reasons:

- lack of an effective hydrogen gas dissolution device and
- safety issues associated with the use of hydrogen.

Both of these concerns can be resolved using a membrane gas transfer device (Semmens, 1991). The membrane system can be used to transfer hydrogen with 100% gas transfer efficiency and bubbleless operation will prevent the release and waste of hydrogen that can lead to explosive conditions in confined spaces.

## 2.4 Membrane Applications in Autorophic Denitrification

Membrane technology was used for simultaneous hydrogen enrichment and denitrification in a single membrane bioreactor (Ho et al., 2001). Hydrogen and carbon dioxide flowed together through the lumen side of a gas-permeable silicone tubular membrane. The gases diffused through the membrane wall directly to a bacterial biofilm attached to the surface of the tube. Hydrogen provided the energy source and carbon dioxide was employed as a carbon source and to neutralize alkalinity resulting from the denitrification.

The silicone tubular membrane of 1.5 mm inside diameter and 2.5 mm outside diameter was wound in coils inside a 1.5-l batch bioreactor. The length of the single tube was 7.5 m. A pure culture of *Ralstonia eutropha* was used for autotrophic denitrification. Feed of synthetic wastewater containing 1 g/L $KNO_3$ was pumped into the bioreactor at 3 ml/min. The hydrogen flow rate was maintained at 20 mL/min. Nitrogen removal rate was between 1.6 and 5.4 g N/d per $m^2$ of membrane area and varied with the carbon dioxide concentration. The maximum rate of nitrogen removal occurred when the carbon dioxide concentration ranged from 20% to 50%. No nitrite accumulation was observed.

A single membrane bioreactor where bacteria were entrapped in the membrane material was employed for nitrification-denitrification (Uemoto and Saiki, 2000). Hydrogen flowed through the lumen side of a single membrane tube immersed in a 0.2 L batch bioreactor containing ammonia solution of 0.472 g of ammonium sulfate agitated vigorously. Nitrification with immobilized *Nitrosomonas europaea* occurred on the outside surface of the membrane tube where aerobic conditions prevailed. Oxygen concentration in the membrane decreased along the wall thickness resulting in anoxic

conditions near the tube lumen. *Paracoccus denitrificans* was employed to carry out denitrification in this region of the membrane. An average nitrogen removal rate of 4.458 g $NH_3$-N/d per $m^2$ of the external membrane surface was achieved.

Autotrophic denitrification with hydrogen-oxidizing bacteria was carried out in a hollow-fiber membrane biofilm reactor (HFMBR) (Ergas and Reuss, 2001). Hydrogen gas was transferred through hollow fiber membranes directly to a bacterial culture to accomplish biological denitrification of drinking water. A hollow fiber membrane module was used in a flow-through configuration. A hydrogen-oxidizing denitrifying biofilm was attached to the outside of the hollow fiber membranes. Water contaminated with nitrate was recycled through the shell side. Nitrate diffused from the bulk fluid to the bacterial culture which converted it to nitrogen gas, effectively denitrifying the water. Hydrogen gas was pumped through the lumen of the fibers and diffused through the membrane to the bacterial culture.

A bench scale HFMBR utilized 2,400 polypropylene hollow fibers with an inner diameter of 200 μm, an outer diameter of 250 μm and a 0.05 μm pore size. A hydrogen oxidizing denitrifying culture was enriched from a wastewater seed. The nitrate loading rate was gradually increased over a three-month period following a 70-day start-up period. The nitrate utilization rate reached 770 g $NO_3$-N/$m^3$day at an influent nitrate concentration of 145 mg $NO_3$-N/L. The hydraulic residence time was 4.1 h. Trial runs with contaminated water from the Cape Cod aquifer resulted in an increase in effluent water dissolved organic carbon (DOC) concentration and turbidity.

HFMBR technology was first applied to hydrogenotrophic denitrification by Lee and Rittmann (2000). The shell and tube configuration was used. Hollow fiber

membranes used were composite membranes manufactured by Mitsubishi Rayon (Model MHF 200TL). The outer and inner layer of the fiber membrane wall were microporous polyethylene. A 1-micron thick layer of non-porous polyurethane was sandwiched between the inner and the outer layers. The non-porous layer allows for high pressure use without premature bubble formation. The modules were comprised of 83 hollow fibers with total gas transfer area of 750 $cm^2$. The total reactor volume was 420 ml. The hollow fiber membrane bundle was housed in a 1.5 cm ID PVC tube in an upflow configuration. The hollow fibers were sealed on one end and were pressurized with hydrogen gas on the other end. Hydrogen gas supplied from a pressurized gas tank at 0.31 atm and 0.42 atm diffused through the membranes into the water stream flowing concurrently on the outside of the membranes.

The outer wall of each fiber membrane was coated with a biofilm. The organism was *Ralstonia eutropha*, a hydrogen oxidizing bacteria. The feed solution of tap water with a nitrate, bicarbonate and 10 mM phosphate was pumped in the shell side of the module with a hydraulic retention time of 42 minutes. Nitrate diffused into the biofilm from the bulk liquid side of the biofilm, while hydrogen was delivered from the fiber side. 76% nitrate removal was achieved at the hydrogen pressure of 0.31 atm and 92% removal was achieved of 0.42 atm. High steady state nitrate fluxes of 0.08 and 0.1 mg $N/cm^2$-d were achieved at the dissolved hydrogen concentration of 0.009 and 0.07 mg $H_2$/l in the effluent. The biofilm thickness was 179 μm.

Hollow fiber membranes have also been used for other gas transfer to biofilms in nitrification-denitrification. HFMBR was effectively used in ammonia removal by nitrification where air was blown through the membranes to supply oxygen to the

nitrifying biofilm (Keskiner and Ergas, 2000). A hollow fiber membrane biofilm reactor was used to treat 2,4,6-trinitrophenol as the sole carbon source. Pure oxygen was fed from the membranes to the biofilm attached to the outer surface of the membrane (Jimenez et al., 1998). Brindle et al. (1998) developed a nitrification process using a hollow fiber membrane reactor where a nitrifying biofilm was attached to the surface of oxygen-permeable hollow fiber membranes. Nitrogen removal of 98% from the nitrogen loading of 1.2 kg $NH_4$-N/$m^2$d at the rate of 6.6 g $NH_4$-N/$m^3$d was accomplished.

Membrane bioreactors effectively eliminate the need for post-treatment associated with biological denitrification. Since nitrate removal requires addition of bacteria, carbon source and buffering salts such as bicarbonate and phosphorus to the water to be treated, residual amounts of these chemicals raise the cost of post-treatment of denitrified water. If carbon dioxide is used as a carbon source, the treated water's pH rises, again adding to the post treatment costs. Membranes show potential to eliminate the problem of drinking water contamination by utilizing their separation capabilities along with gas transfer characteristics. Fuchs *et al.* (1997) separated the biological reaction zone and carbon supply from the raw water stream by a nitrate permeable membrane. Nitrate diffused from the water through the membrane into the biofilm while carbon and phosphate were transferred to the bacteria on the biofilm side of the membrane. In effect, the effluent was not contaminated with residual bacteria and chemicals because the membranes separated the two solutions. Cellulose dialysis membrane tubing (7.5 mm I.D.) was used with a mixed heterotrophic culture. A denitrification rate of 1230 mg $NO_3$-N/$m^2$d was achieved in this configuration. Without post-treatment, the effluent met nearly all criteria for drinking water.

Hoerner and Irmer (1989) applied the membrane fluidized-bed technology to autortophic denitrification. The method combines the advantages of a fluidized bed (i.e., optimal mass transfer conditions combined with very high biomass concentration on fine grained carrier particles with a very high volumetric surface) in excluding any clogging, and the optimal bubble-free gas intake through permeation membranes. Hydrogen and carbon dioxide concentrations and pH are constant because of even distribution in the whole fluidized bed volume. Therefore, optimal conditions are available to microorganisms in the whole reactor resulting in very high specific denitrification rates. The achievable reaction rate essentially depends on the kind and the quantity of the carrier particles and on the rate of the hydrogen intake. At limiting hydrogen rates or carrier limitation a maximum reaction rate is obstructed which is independent of nitrate load. A pilot plant was operated at retention times of about 15 min. Denitrification rates of 2.5 kg $NO_3$-N/$m^3$d were obtained over longer periods for hydrogen limited operation, which can be further increased by increasing the membrane surface or membrane permeability. The membrane fluidized-bed technology is applied to autotrophic denitrification in Wurzen waterworks (Germany).

Biologically treated wastewater was effectively denitrified in a fluidized bed using hydrogen as electron donor when the hydrogen was introduced through silicone rubber tubular membranes with specific area of 120 $m^2/m^3$ (Brautigam and Sekoulov, 1987). The denitrification rate was 60 g $NO_3$-N/$m^3$-h at hydrogen partial pressure of 2 bar. Over time, biological growth on the membrane decreased the denitrification rate to 30 g/$m^3$-h.

Membrane dissolution of hydrogen for autotrophic denitrification was investigated by Gantzer (1995). The study used a hollow fiber membrane system to supply high dissolved hydrogen concentration in a fixed-bed denitrification bioreactor. The hydrogen gas was maintained at a pressure of 2 atm inside the fibers. As shown in Table 1, the nitrate removal rate of the autotrophic process was found to be much higher than that of a heterotrophic process. The steady state nitrate flux into the fixed-bed biofilms averaged about 85 mg $NO_3^-$–N/$m^2$/hr, which is much higher than the denitrification rates reported in the literature. Although the author stated that the process (i.e., the biofilm) was nitrate limited, no experiment was conducted to verify this claim. Based on data reported by various researchers, it appears that the process is "liquid phase hydrogen concentration limited", which is in contrast with the results of Kurt et al. (1987).

## 2.5 Modeling of Denitrification Kinetics

Literature concerning the subject of kinetics modeling of nitrate removal is limited. Some attempts were documented where overall nitrogen removal and cell growth were modeled in heterotrophic systems. However, the reported models do not provide a thorough analysis of the denitrification process since they do not account for nitrite generation. This section focuses on models which include intermediate formation in autotrophic and heterotrophic nitrate removal processes.

### 2.5.1 Modeling of Autotrophic Denitrification

Kurt et al. (1987) studied the biodegradation kinetics of autotrophic hydrogen oxidizing bacteria modeling the process using a double Michaelis-Menten function. Nitrate, nitrite and hydrogen were assumed to be limiting substrates in a bench scale fluidized bed reactor. Nitrate and hydrogen were assumed to be limiting substrates in the first denitrification step, and nitrite and hydrogen were assumed limiting in the second step. The following equations were used:

$$r_I = V_{mI} \frac{C_{NO3}}{K_{NO3} + C_{NO3}} * \frac{C_{H2}}{K_{I,H2} + C_{H2}} \quad (2.1)$$

$$r_{II} = V_{mII} \frac{C_{NO2}}{K_{NO2} + C_{NO2}} * \frac{C_{H2}}{K_{II,H2} + C_{H2}} \quad (2.2)$$

where $r_I$ and $r_{II}$ are reaction rates of reaction 1.1 and 1.2 respectively (mg/L-h); $V_{mI}$ and $V_{mII}$ are maximum rate constants (mg/L-h); C is the liquid phase substrate concentration (mg/L); and K is the saturation constant (mg/L). The denitrification rate was shown to be more strongly dependent on the nitrate concentration than on hydrogen. Although hydrogen is only slightly soluble in water (1.6 mg/L at 20°C), the saturation constants for hydrogen were reported to be less than 1% of saturation. Therefore, it is evident that the liquid phase hydrogen concentration has very little effect except at low nitrate concentrations. The Michaelis-Menten model does not include biomass growth and thus does not provide the complete representation of the biological process.

### 2.5.2 Modeling of Heterotrophic Denitrification

Peyton et al. (2001) investigated biological kinetics of a heterotrophic denitrification process under high pH and high salinity conditions. The model employed first-order kinetics with respect to nitrate and nitrite as follows:

$$\frac{dC_{NO_3}}{dt} = - k_1 C_{NO_3} X \tag{2.3}$$

$$\frac{dC_{NO_2}}{dt} = k_1(0.7419)\, C_{NO_3} X - k_2 C_{NO_2} X \tag{2.4}$$

where $k_1$ and $k_2$ are reaction rate constants (L/h-mg) and C and X are substrate and cell concentrations (mg/L), respectively. Cell growth rate was modeled as a sum of nitrate removal rate and nitrite change multiplied by respective cell yields. This model adequately describes the kinetics of the heterotrophic system by accounting for both intermediate and cell generation rates. Subsequently, nitrate utilization rate and cell yield were determined based on kinetic coefficients to compare the behavior of the system to other denitrification processes.

Nitrate and nitrite were modeled using first-order kinetics in heterotrophic denitrification with methanol as a carbon source (Smith et al., 1993). The equations used are given below:

$$\frac{dC_{NO_3}}{dt} = - k_1 C_{NO_3} \tag{2.5}$$

$$\frac{dC_{NO_2}}{dt} = k_1 \beta\, C_{NO_3} - k_2 C_{NO_2} \tag{2.6}$$

where β is a dimensionless constant which accounts for the empirical observation that less than one mole of nitrite appears in solution for each mole of nitrate reduced. It takes place of the stoichiometric ratio of 0.7419 in equation 2.4. However, cell growth was not accounted for as in the case of Kurt et al. (1987) discussed earlier. The researchers make a claim that (1-β) fraction of bacteria is capable of reducing nitrate and nitrite in one operation and the remainder reduces nitrite to nitrogen. This conclusion is in disagreement with the majority of denitrification literature which affirms that nitrate to nitrogen gas reduction is carried out by one bacterial species under heterotrophic conditions (Metcalf and Eddy, 1993; Rittmann, 2002).

## 2.6 Research Needs

Autotrophic hydrogen oxidizing bacteria can be used for denitrification. These bacteria use carbon dioxide or bicarbonate for cell synthesis. Hydrogen is used as the energy source and electron donor while nitrate acts as the electron acceptor.

The growth rate of autotrophic bacteria is typically slower than heterotrophic bacteria. Therefore, lower concentrations of biomass and soluble microbial products can be expected in the reactor effluent. A comprehensive model for cell growth and nitrate and nitrite utilization is needed to better describe the process. The advantages of this process over conventional heterotrophic denitrification can be summarized as follows:

- No addition of organic carbon for cell synthesis,
- No interferences with the disinfection process (no disinfection byproduct formation),
- The process can be operated as a fixed or fluidized bed reactor,

- The process is cost effective compared to methanol, ethanol or acetate as carbon sources.

The fact that hydrogen gas is inherently clean makes it the ideal reactant to denitrify drinking water. Hydrogen generates less excess biomass than the use of organic compounds, and if generated on-site is less expensive than the use of methanol, ethanol, and acetate based on bulk chemical cost. The concerns for safety and lack of gas dissolution devices for hydrogen can be resolved using a membrane gas transfer device. A membrane system can be used to dissolve hydrogen in water with 100% gas transfer efficiency and the systems' bubbleless operation can prevent the release and waste of hydrogen that can lead to explosive conditions in confined spaces.

This research therefore addresses the feasibility of a novel membrane process for hydrogen gas transfer for autotrophic denitrification.

**Table 2.1: Comparison of Nitrate Removal Rates**

| Electron Donor | Nitrate removal rate (mg $NO_3$-N/$m^2$-hr) | Reference and Experimental Conditions |
|---|---|---|
| Methanol | 10 | Liessens et al., 1993. Biofilm reactor, Methanol. |
| Hydrogen | 13 | Kurt et al., 1987. Biofilm reactor (sand), Hydrogen at 1 atm. |
| Hydrogen | 33 | Islam et al., 1994. Biofilm reactor, Hydrogen at 1 atm. |
| Hydrogen | 58 | Benedict, 1996. Biofilm reactor, Hydrogen at 1 atm. |
| Hydrogen | 85 | Gantzer, 1995. Biofilm reactor, Hydrogen at 2 atm. |

# CHAPTER 3

# BATCH REACTOR STUDIES FOR BIOLOGICAL KINETICS EVALUATION

## 3.1Introduction

Batch autotrophic denitrification experiments were carried out using an acclimated mixed bacterial culture obtained from a local wastewater treatment plant. Inorganic carbon was delivered via sodium carbonate of carbon dioxide, while hydrogen gas was supplied as the electron donor. Anoxic conditions were maintained so that nitrate acted as the electron acceptor. A number of common genera of soil bacteria are able to use hydrogen as an electron donor and inorganic carbon for cell synthesis. Bacteria such as *Pseudomonas pseudoflava*, *Ralstonia eutropha* and *Paracoccus denitrificans* have the ability of autotrophic denitrification using hydrogen gas as the electron donor (Schmidt et al., 1989; Selenka and Dressler, 1990). The chemical reactions of nitrate reduction by hydrogen oxidizing bacteria has been shown by Kurt et al., (1987) as follows:

$$2NO_3^- + 2H_2 \rightarrow 2NO_2^- + 2H_2O \quad (3.1)$$

$$2NO_2^- + 3H_2 \rightarrow N_2 + 2H_2O + 2OH^- \quad (3.2)$$

Combining reactions (3.1) and (3.2), the overall reaction can be written as:

$$2NO_3^- + 5H_2 \rightarrow N_2 + 4H_2O + 2OH^- \quad (3.3)$$

Thus stoichiometrically, 0.35 mg/L of hydrogen is required for complete denitrification of 1.0 mg $NO_3^-$ N/ L. However the dentrification kinetics of autotrophic denitrification is not well established. Knowledge of microbial growth and substrate utilization characteristics is important in design of biological unit processes and in the predication of the fate of compounds in natural and engineered environments. Therefore it is important that realistic values for biodegradation kinetic coefficients be used in fate and transport models.

Batch experiments help in characterizing the kinetic parameters related to cell growth. Therefore batch studies were conducted in the laboratory with the following objectives:

- *develop* an acclimated mixed culture capable of autotrophic denitrification using hydrogen as an electron donor,
- *monitor* nitrate, nitrite and cell mass concentration with time, and
- *model* the biodegradation kinetics of the batch autotrophic denitrification process.

## 3.2 Materials and Methods

### 3.2.1 Source of the Culture

A mixed culture was obtained from the anoxic denitrification basin of the Winslow Wastewater Treatment Plant (Winslow, NJ). An acclimated culture for autotrophic denitrification using hydrogen oxidizing bacteria was developed in batch reactors at room temperature in five passages.

### 3.2.2 Kinetic Experiments

Sodium carbonate ($Na_2CO_3$) and sodium nitrate ($NaNO_3$) were obtained from Sigma Chemicals Co., St. Louis, MO. HACH BOD nutrient buffer pillows (HACH Chemical Company, Loveland, CO.) amended with excess phosphate buffer (Ergas and Reuss, 2001) were used for the growth media. High purity hydrogen and carbon dioxide gas were obtained from MG Gas Industries (Malvern, PA). Deionized distilled water from a Barnstead Water Purification Water System (Dubuque, Iowa) was used for preparation of all solutions.

The experimental setup for the batch studies is presented in Figure 3.1. Glass amber jars (4 L) with magnetic stir bars for adequate mixing were used as the reactors. Two sets of batch studies were conducted with two different inorganic carbon sources: carbonate and carbon dioxide gas.

#### *Carbonate Studies*

Four batch reactors were used in this study. Each batch reactor received 100 mg/L of $Na_2CO_3$ and 100 mg/L of $NO_3^-$. Therefore the reactors had a concentration of 25 mg/L $NO_3$ –N. The reactors were seeded with 4 mL of mixed liquor from an acclimation reactor containing bacteria acclimated to carbonate as their sole carbon source. The control reactor did not receive any mixed liquor. The reactors were purged with hydrogen gas every 4 hours with the aid of solenoid valves (Model 6013A, Burkert, Orange, CA), which were controlled by programmable timers (Model XT, ChronTrol Corp., San Diego, CA). The gas lines were fitted with check valves to prevent back flow of gas. A stir bar continuously mixed the reactor contents. Samples were analyzed for

nitrate, nitrite, cell mass, pH and alkalinity with time. Experiments were conducted under a fume hood and in duplicate.

***Carbon Dioxide Studies***

Four batch reactors were also used in this study. A carbon dioxide based acclimation reactor was started using seed from the $Na_2CO_3$ acclimation reactor. The reactors were purged every 4 hours with $H_2$ gas and every 10 hours with $CO_2$ gas through a bubble-stone. The gas cycling was controlled with the aid of solenoid valves (Model 6013A, Burkert, Orange CA) and a programmable timer (Model XT, ChronTrol Corp., San Diego, CA).

### 3.2.3 Analytical Methods

The following parameters were monitored during the course of the batch experiments: pH, alkalinity, nitrate, nitrite and cell mass. Nitrate and nitrite were measured using the Standard Method 4500-B (AWWA *et al.*, 1995) and HACH Method 8153, on a HACH DR 4000U (Loveland, CO) spectrophotometer. pH was measured with an Orion 720 pH Meter (Beverly, MA). Alkalinity was determined using a HACH digital titrator according to Standard Method 2130 B (Standard Methods 1995; 2130 B). Dissolved oxygen concentrations were measured with a YSI 520 DO Meter (YSI, Yellow Springs, CO). Cell mass was measured as protein and MLSS (Mixed Liquor Suspended Solids). Protein measurements were made according to the method of Lowry et al. (1951). Bovine serum albumin (Sigma Chemicals, St. Louis, MO) was used as the protein standard. Cell mass as MLSS was measured according to Standard Method

(AWWA *et al.*, 1995). TOC and DOC measurements were also made using HACH Method 8153 on a HACH DR 4000U (Loveland, CO) spectrophotometer.

### 3.2.4 Modeling

Since autotrophic denitrification is a relatively new process, few modeling attempts are reported in literature. The existing models simplify the system by ignoring response variables such as intermediate nitrite accumulation or cell mass. Thus, current literature lacks a more representative model, which is needed to better understand the biological kinetics.

In this study, the conventional Monod model (Monod, 1943; Rittmann, 2002) was used to model experimental data. The model was used to describe the rate of nitrate removal, nitrite accumulation and cell growth. Nitrate is removed from the system by microorganisms according to the following relationship:

$$\frac{dC_{NO_3}}{dt} = -\frac{1}{Y_{NO_3}} \frac{\mu_{m1} C_{NO_3} X}{K_{NO_3} + C_{NO_3}} \tag{3.4}$$

where $\frac{dC_{NO_3}}{dt}$ = nitrate conversion rate, mg $NO_3$-N/L-hr

$C_{NO_3}$ = nitrate concentration, mg $NO_3$-N/L

X= cell concentration, mg/L

$\mu_{m1}$ = maximum specific growth rate for reaction 3.1, $hr^{-1}$

$K_{NO_3}$ = nitrate half velocity constant, mg $NO_3$-N /L

$Y_{NO_3}$ = yield coefficient, mg cells formed/mg $NO_3$-N converted

Nitrate is converted to nitrite which itself is further biodegraded. Hence, the nitrite concentration change with time is given by:

$$\frac{dC_{NO_2}}{dt} = \frac{1}{Y_{NO_3}} \frac{\mu_{m1} C_{NO_3} X}{K_{NO_3} + C_{NO_3}} - \frac{1}{Y_{NO_2}} \frac{\mu_{m2} C_{NO_2} X}{K_{NO_2} + C_{NO_2}} \qquad (3.5)$$

where $\frac{dC_{NO_2}}{dt}$ = nitrite conversion rate, mg $NO_2$-N/L-hr

$C_{NO_2}$ = nitrite concentration, mg $NO_2$-N/L

$\mu_{m2}$ = maximum specific growth rate for reaction 2.2, $hr^{-1}$

$K_{NO_2}$ = nitrite half velocity constant, mg $NO_3$-N /L

$Y_{NO_2}$ = yield coefficient, mg VSS formed/mg $NO_2$-N converted

Finally, cells are produced both during nitrate removal and nitrite production and uptake. Therefore, the rate of cell growth may be described as:

$$\frac{dX}{dt} = Y_{NO_3} \frac{dC_{NO_3}}{dt} + Y_{NO_2} \frac{dC_{NO_2}}{dt} - k_d X \qquad (3.6)$$

where $\frac{dX}{dt}$ = net rate of bacterial growth, mg VSS/L-hr

$k_d$ = decay coefficient, $hr^{-1}$

The following assumptions were made in model development:

- preacclimated microorganisms;
- growth is only nitrate limited;
- nutrients are available in excess;
- cell growth conditions are optimum;
- no inhibition occurs.

Hydrogen was assumed to be not limiting as evidenced by previous investigations (Kurt et al., 1987).

The above kinetic equations were solved simultaneously numerically for $C_{NO3}$, $C_{NO2}$ and X using a sixth-order Runge-Kutta method in POLYMATH ODE solver. A search for the values of the kinetic parameters will be carried out using an algorithm for least squares estimation. This algorithm finds a local minimum of the sum of the square weighted errors (SSWE).

## 3.3 Results and Discussion

Results from batch studies conducted with carbonate as the sole carbon source are presented in Figure 3.2. Nitrate removal was almost complete in two days. Nitrite concentration indicates some accumulation but complete removal during the duration of the experiment. Other researchers (Kurt and Dunn, 1987; Oh et al, 1999; Miyake et al., 1996; Smith et al., 1993) have reported nitrite accumulations during batch autotrophic denitrification studies. All authors suggested that a continuous flow process having a relatively long retention time would result in complete nitrogen removal. Cell mass, pH

and alkalinity concentrations for these experiments are presented in Figures 3.3, 3.4 and 3.5. The buffering capacity in the reactors seems adequate from these results.

Results from the batch experiments with $CO_2$ as the source of carbon delivery were very similar to those obtained from the carbonate tests. Results for Nitrate, Nitrite, Cell Mass, pH and alkalinity are presented in Figures 3.6 through 3.9. In both systems the total carbonate distribution between $H_2CO_3$ and $HCO_3^-$ would have to be similar because the system pH were analogous. This would explain the comparable nitrate and nitrite removal in both sets of experiments. The only difference noted was in cell mass measurement techniques. Protein measurements worked well with the $CO_2$ system while suspended solids measurements worked for the sodium carbonate system. Cell mass as protein was analyzed according to the method of Lowry et al. (1951). Protein concentrations were analyzed as problems were encountered for representative cell mass concentration as MLSS. Hydrogen concentrations were measured intermittently during the course of these experiments. Hydrogen concentration was found to be 62.5% of saturation (1.6 mg/L) in both systems. This indicates that the process was not hydrogen limited. All batch studies indicated that rapid nitrate removal is possible with autotrophic denitrifiers. Nitrite accumulations occurred but were removed during the course of these experiments.

Modeling results are presented in Figure 3.10. The kinetic coefficients obtained from this study are summarized in Table 3.1 The substrate utilization rate for autotrophic denitrification was determined to be 1.0 mg $NO_3$-N/mg VSS-day. It was calculated by combining the kinetic coefficients with equation 3.4 at a nitrate concentration of 10 mg $NO_3$-N/L. The autotrophic denitrification rate is higher than those reported for

heterotrophic denitrification, 0.01-0.6 mg $NO_3$-N/mg VSS-day (USEPA, 1993; Peyton, 1994). The obtained value is also higher than heterotrophic denitrification rate of 0.4 – 0.7 mg $NO_3$-N/mg VSS-day reported under high salinity/ high pH conditions with first-order kinetics describing the system behavior (Peyton et al., 2001). Thus, less biomass is needed to remove the same amount of nitrate. This result indicates that autotrophic denitrification has a significant potential to compete with heterotrophic processes for nitrate removal.

Biomass yields were obtained to estimate the amount of biomass produced during nitrate and nitrite removal in autotrophic denitrification. Since yield values are usually reported for complete removal of nitrate to nitrogen gas, overall yield coefficients were calculated for design and scale up purposes. The overall cell yield was 0.78 mg VSS/mg $NO_3$-N. Table 3.2 provides a comparison to literature values for heterotrophic and sulfur reducing conditions. Benedict et al. (1996) reported a similar biomass yield of 1.2 mg VSS/mg $NO_3$-N. The obtained cell yield is in the range of heterotrophic values (Metcalf and Eddy, 1991). Therefore, excessive biomass generation is not expected in system operation.

## 3.4 Conclusions

These studies indicate the presence of hydrogen oxidizing denitrifiers in wastewater treatment plants. A mixed culture capable of utilizing both carbonate and $CO_2$ as the sole carbon source could be developed having the ability of using hydrogen as an electron donor. Adequate pH control was possible and the pH averaged around 6.6. High nitrate utilization rate affects denitrification design resulting in shorter retention

times and smaller reactor volumes. Less biomass generation is expected in operation of the process than in sulfur reduction systems.

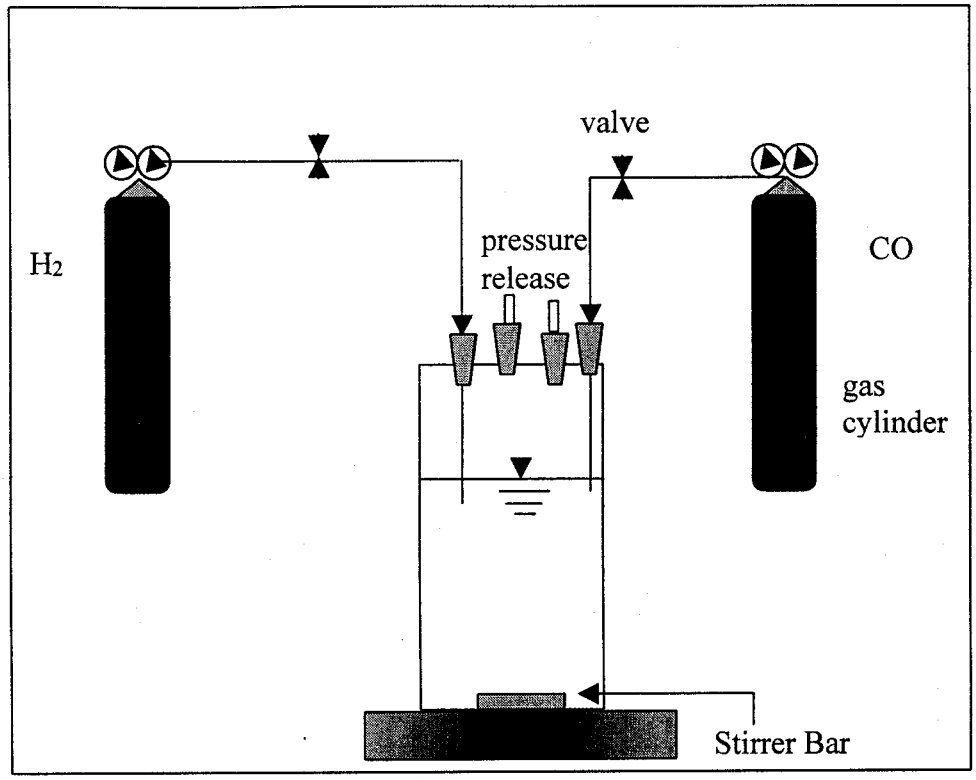


**Figure 3.1: Experimental set-up for batch studies**

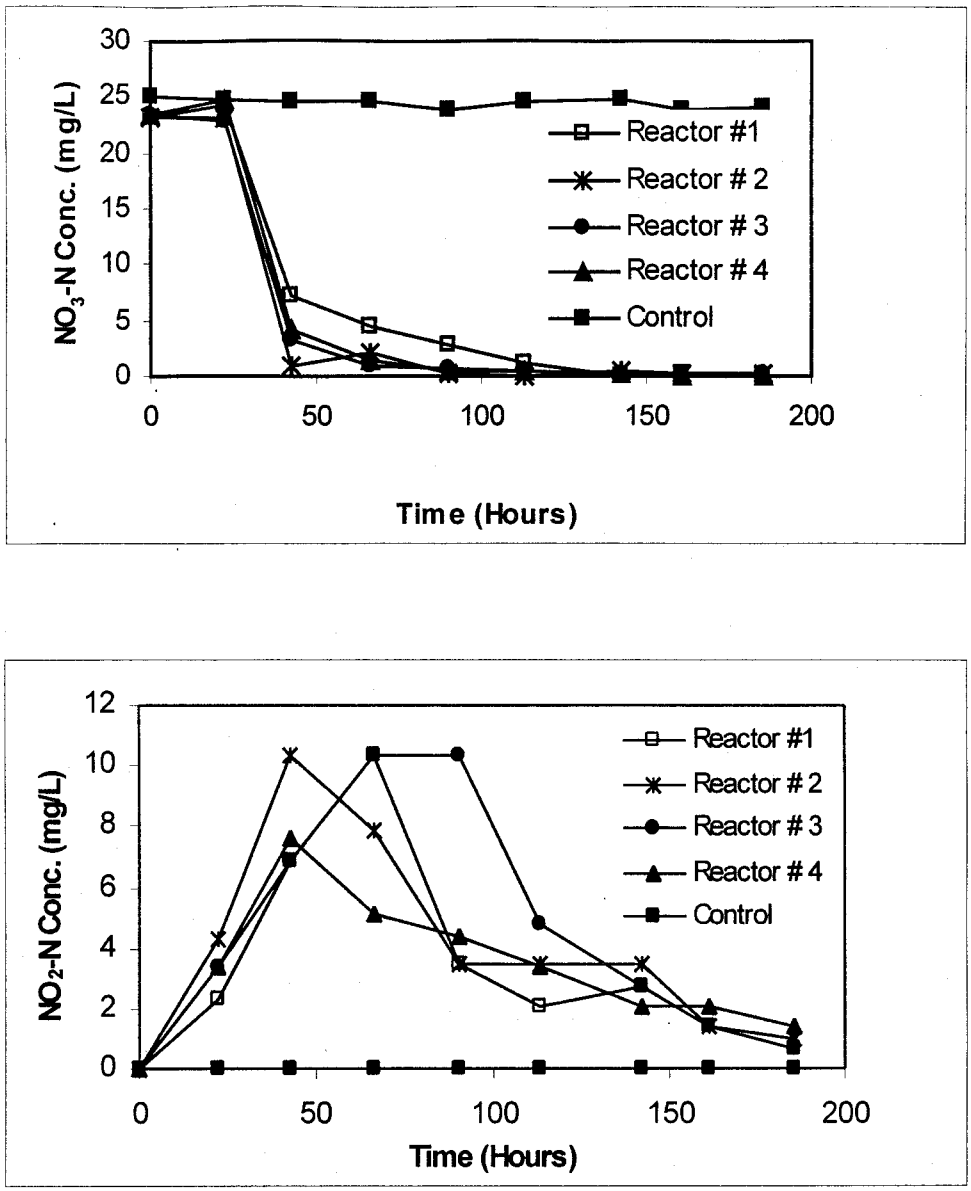


**Figure 3.2: Nitrate and nitrite removal in batch reactors with sodium carbonate**

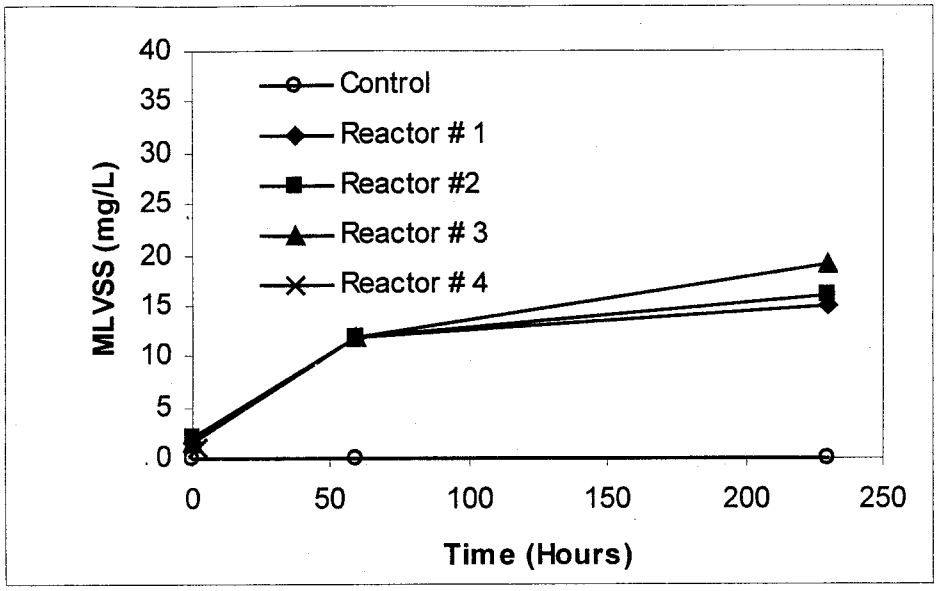


**Figure 3.3: Cell mass concentration with time in batch reactors with sodium carbonate**

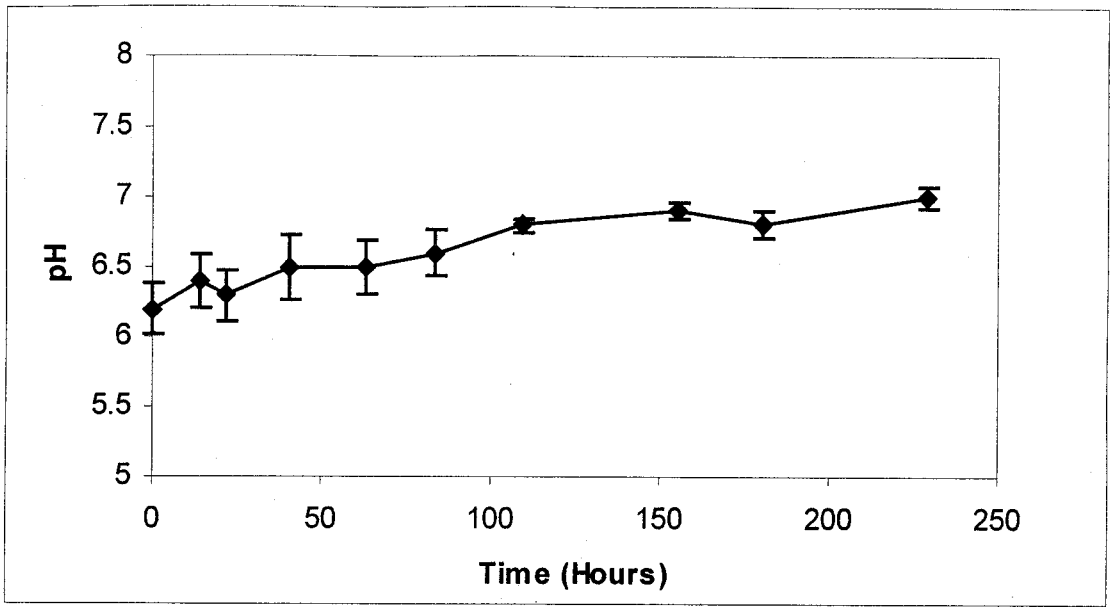


**Figure 3.4: pH changes with time in batch reactors with sodium carbonate**

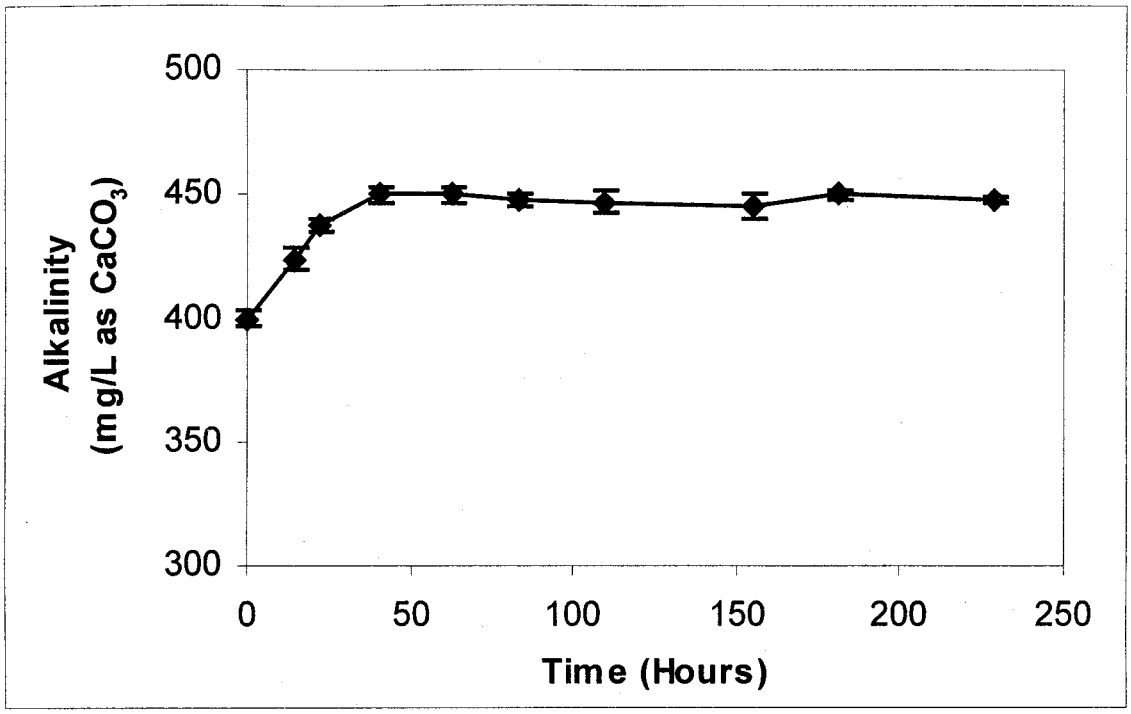


**Figure 3.5: Alkalinity changes with time in batch reactors with sodium carbonate**

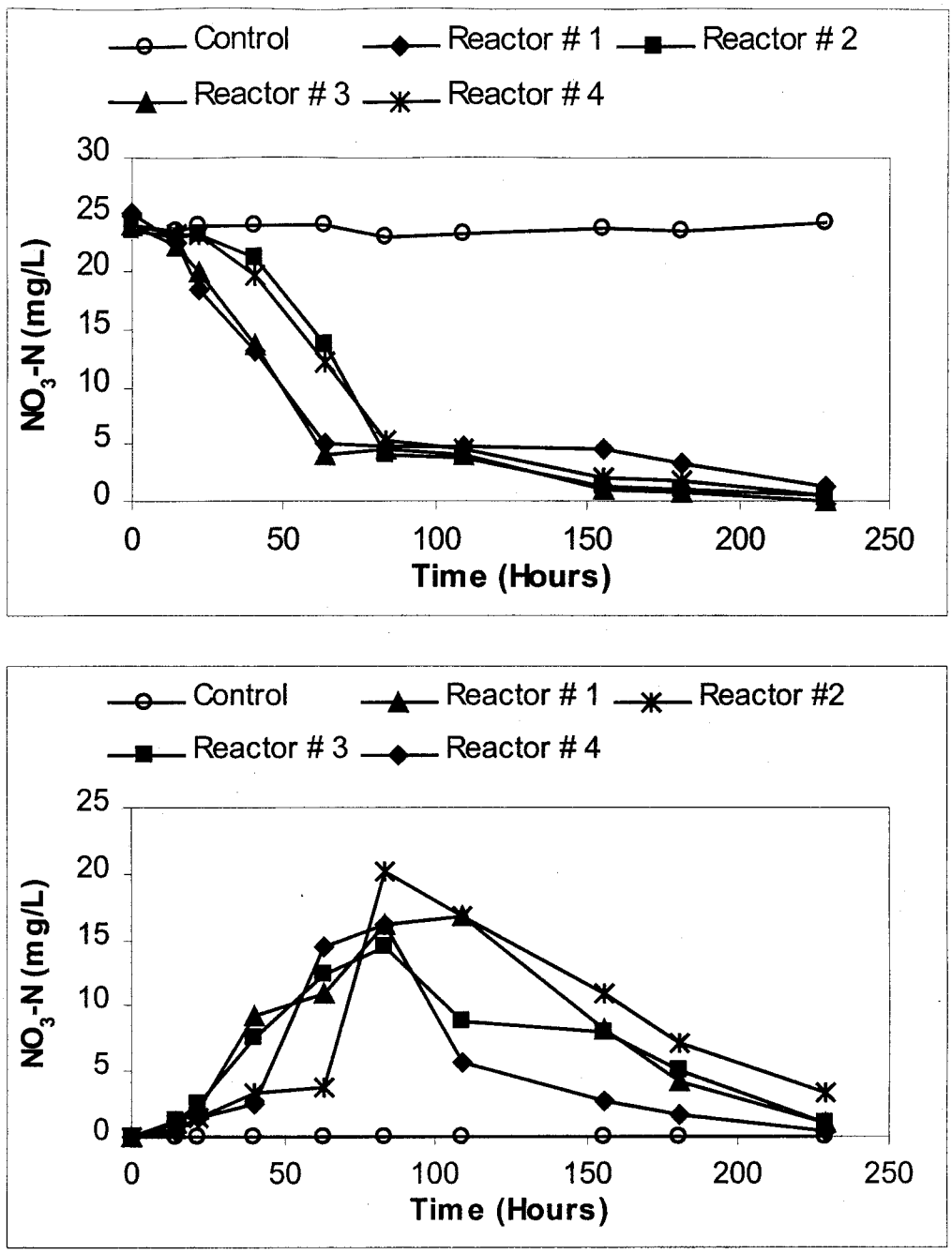


**Figure 3.6: Nitrate and nitrite concentration with time in batch reactors with $CO_2$**

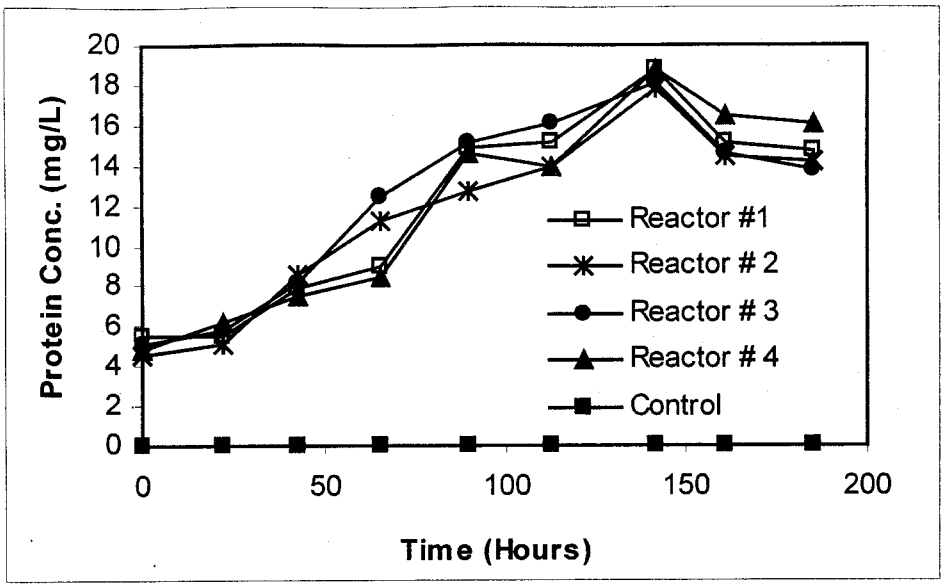


**Figure 3.7: Cell Mass Concentration with Time in Batch Reactors with $CO_2$**

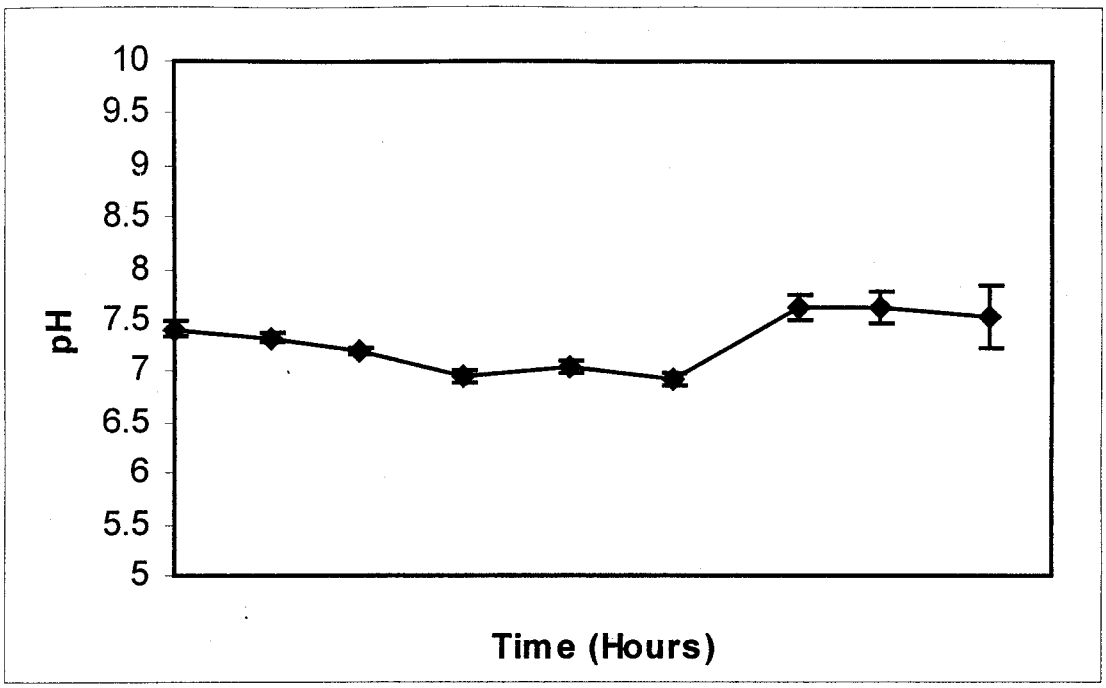


**Figure3.8: pH Changes with Time in Batch Reactors with $CO_2$**

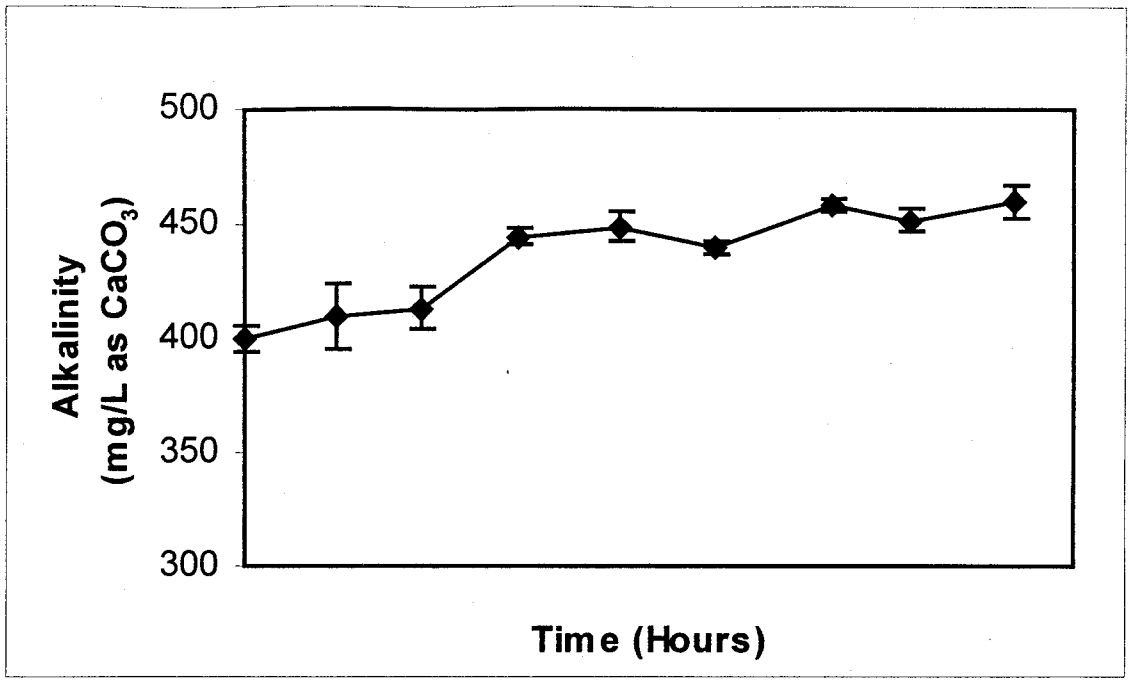


**Figure 3.9: Alkalinity Changes with Time in Batch Reactors with $CO_2$**

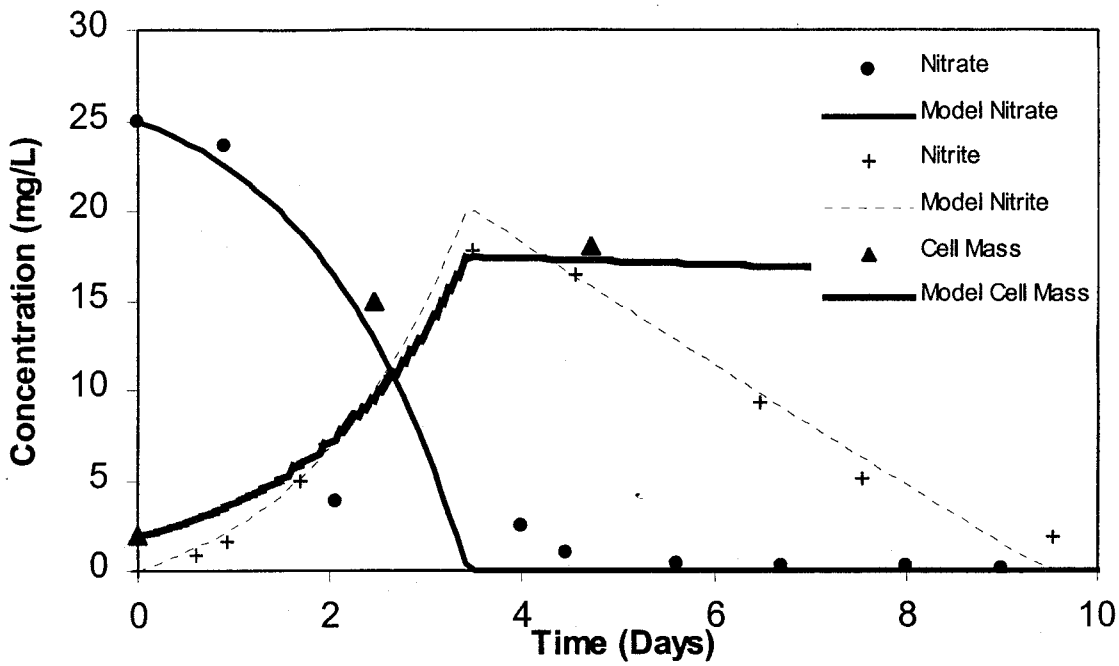


**Figure 3.10: Model predictions for autotrophic denitrification**

**Table 3.1: Summary of Kinetic Parameters for Autotrophic Denitrification**

| Kinetic Parameter | Units | Value |
|---|---|---|
| $\mu_{m1}$ | $day^{-1}$ | 0.65 |
| $\mu_{m2}$ | $day^{-1}$ | 0.03 |
| $K_{NO3}$ | mg/L | 0.1 |
| $K_{NO2}$ | mg/L | 0.1 |
| $Y_{NO3}$ | mg cell/mg $NO_3$-N | 0.63 |
| $Y_{NO2}$ | mg cell/mg $NO_2$-N | 0.15 |
| $k_d$ | $day^{-1}$ | 0.04 |

**Table 3.2: Comparison of Kinetic Parameters for Denitrification**

| Denitrification Type | $\mu_m$ 1/day | Y mg cell/ mg $NO_3$-N | $K_s$ mg/L | $k_d$ 1/day | Reference |
|---|---|---|---|---|---|
| Heterotrophic | 0.3-0.9 | 0.4 -0.9 | 0.06-0.20 | 0.04-0.08 | Metcalf and Eddy, 1991 |
| Autotrophic** | 2.88-4.8 | 0.4-0.5 | 3-10 | 0 | Oh et al., 2000 |
| Autotrophic** | 2.64 | 0.57 | 0.2 | 0 | Claus and Kutzner, 1985 |
| Autotrophic* | 0.77 | 1.2 | 0.1 | 0 | Benedict, 1996 |
| Autotrophic* | 0.65 | 0.78 | 0.1 | 0.04 | This Study |

* Hydrogen Oxidizing Bacteria ** Sulfur bacteria

# CHAPTER 4

# HYDROGEN TRANSFER VIA HOLLOW FIBER MEMBRANES

## 4.1 Introduction

Hydrogen transfer into water is needed in certain water and wastewater treatment processes, where hydrogen is required as an electron donor, such as autotrophic denitrification. In recent years hydrogen transfer has also become important in natural attenuation (USEPA, 1998) and in-situ biodegradation of organic pollutants (Novak et al., 2001). The advantages of using hydrogen over conventional organic energy sources are that it is less expensive and does not leave an organic residue in the treated water. However, the use of hydrogen has been limited because of a safety issue associated with conventional sparging of hydrogen into water (formation of bubbles presents an explosion hazard). Hollow fiber membranes may be used for bubbleless hydrogen-to-water transfer.

### 4.1.1 Membrane Selection

Hydrogen gas transfer into water may be accomplished through porous or non-porous membranes. Asymmetric membranes which consist of a porous and non-porous layer may also be used. In order to obtain high hydrogen transfer rates, the membrane material must be (1) able to withstand high pressures, (2) highly hydrogen permeable, and (3) thin enough to be made into small diameter hollow fibers.

Microporous hydrophobic membranes have the advantage of very high gas permeabilities. Since the pores are gas-filled, diffusion takes place rapidly in the gas phase. These membranes are available as small-diameter (200-400 μm) hollow fibers that provide a very high specific surface area (i.e., surface area to volume ratio). The use of porous membranes is limited to low pressure applications because high pressures result in bubble formation. Nevertheless, they have found applications in absorption and water treatment. Hydrogen mass transfer was achieved through Teflon hollow fiber membranes as a valid alternative to absorption tower operation (Iversen et al., 1995). Microporous hollow fiber membranes were applied in hydrogen gas scrubbing and absorption (Li et al., 2000). More recently, hydrogen was transferred through hollow fiber membranes directly to a bacterial culture for biological denitrification of drinking water (Ergas and Reuss, 2001).

Non-porous membranes such as silicone rubber may be operated at elevated gas pressures without bubble formation. Gas transfer is accomplished via solution-diffusion mechanism. Hydrogen first dissolves in the membrane material and subsequently diffuses through the membrane to the liquid. Brautigam and Sekoulov (1987) introduced hydrogen to water through silicone rubber tubular membranes for the purpose of biologically treating wastewater through denitrification in a fluidized bed with hydrogen as the electron donor. There are several disadvantages of non-porous film application in hydrogen transfer. Since non-porous membranes are thicker than porous membranes, they present an increased resistance to mass transfer, and, therefore, reduce hydrogen transfer rate. In addition, non-porous membranes are not available in small diameter (100-400 μm) fiber form.

Anisotropic or asymmetric membranes consist of a thin skin membrane layer cast on top of a thicker porous backing. The thin skin performs the separation, while the thick layer provides mechanical support for high-pressure applications. Sell *et al.* (1993) applied a non-porous polymer composite membrane in hollow fiber configuration for hydrogen transfer. The outer surface of the fibers was composed of a polyetheramide non-porous layer and a microporous skin on the lumen side. The internal skin was coated with PDMS resulting in 1.2 mm outer diameter and 1 mm inner diameter of the hollow tube.

In biological applications, hydrogen gas was transferred to an autotophic denitrifying bacterial biofilm through an asymmetric composite membrane (Lee and Rittmann, 2000). The outer and inner layer was composed of microporous polyethylene with a non-porous polyurethane layer sandwiched between them. As in the case of non-porous membranes, an anisotropic film is comparatively thick which limits its hydrogen transfer characteristics and forces an increase in the diameter of hollow fibers. And lastly, asymmetric hollow fiber membranes are much more expensive than microporous membranes because of an involved spinning and coating manufacturing process.

## 4.2 Membrane Module Design

Gas transfer *via* hollow fiber membrane modules may be accomplished in the flow-through mode or in the sealed-end configuration (Figure 4.1). In the flow-through mode, gas is pumped continuously through the lumen of the fiber. A portion of the gas diffuses through the membrane and the remaining gas is vented off (Yang and Cussler,

1986). In the sealed-end operational configuration, one end of each hollow fiber membrane in the bundle is sealed. Membranes are then pressurized with gas, which diffuses through the membrane into the water.

Ahmed and Semmens (1992) demonstrated that sealed-end operation results in superior performance as compared to the flow-through configuration. Since gas is vented off in the flow-through mode, it is impossible to achieve a 100% gas transfer efficiency. Also, flow-through operation may result in effective stripping of dissolved volatile compounds from the liquid with the venting gas.

Both of those considerations are important to hydrogen gas transfer. Venting hydrogen, which results from flow-through operation, constitutes a safety hazard. Additional costs must be incurred to contain the off gas and to avoid explosion risks when mixed with air. Stripping of compounds such as volatile organic compounds (VOCs) presents a problem in applications of hydrogen transfer to wastewater treatment. VOCs present in wastewater may diffuse through the membrane into the hydrogen stream increasing the cost of subsequent treatment of the off gas. These constraints may be effectively eliminated through sealed-end operation where all hydrogen diffuses into the water through the membrane resulting in 100% transfer efficiency. Elimination of the vent stream reduces the explosion risk hazard and prevents stripping of VOCs.

Thus the use of microporous hollow fiber membranes for hydrogen gas transfer into water was evaluated. A mass transfer correlation for hydrogen was developed in two configurations: sealed-end and flow-through. Experiments were conducted with the following objectives:

- *Construct* hollow fiber membrane modules for hydrogen gas delivery;
- *Evaluate* the effect of various physical and process variables on the mass transfer rate across the membrane system;
- *Determine* the mass transfer coefficient correlation for various operating parameters such as flow and pressure.

## 4.3 Experimental Methods

Schematics of sealed-end and flow-through modules are shown in Figure 4.2. Hollow fiber membranes are potted into a tube to form a shell-and-tube configuration. The potted end is connected to an air-pump. Gas transfer occurs as water is pumped co-currently on the outside of the fibers on the shell side. The turbulence of water flow causes the fibers to fluidize, or flutter independently. This fiber movement within the pipe enhances mass transfer and has a potential to minimize biological and chemical fouling on the outside of the fibers.

Celgard™ X40-200 Microporous Hollow Fiber Membranes (Celgard Inc., Charlotte, NC) were selected for this study. These are thin-walled, opaque, polypropylene membranes with a nominal internal diameter of 200 μm. Nominal porosity of the membrane material is 25% with effective pore size of 0.04 μm and pore dimensions of 0.04 μm x 0.01 μm. The membranes are durable and pressure resistant with burst strength of 400 psi and tensile break strength exceeding 300 g/fiber.

The hollow fiber modules were constructed by potting several fibers into an external shell. The shell consisted of a glass tube fitted with a Y-connector. After one end of each hollow fiber was heat-sealed, the open ends were potted into the Y-connector with an epoxy adhesive (DP-125, 3M, St. Paul, MN) as shown in Figure 4.2. In the flow through configuration, both ends were potted into Y-connectors.

The experimental set-up for sealed-end studies is shown in Figure 4.3. The hollow fiber module was constructed by potting six fibers into an external shell, 125 cm in length and 0.406 cm in diameter. The water was pumped from a 2.5-L closed reservoir to the hollow fiber membrane module by a peristaltic pump (Model 7553-70, Cole-Parmer, Vernon Hills, IL). The water flow rate was monitored with a turbine flow meter (Model 32919-25, Cole-Parmer, Vernon Hills, IL). High purity hydrogen, obtained from MG Gas Industries (Malvern, PA), was supplied from a gas cylinder and the pressure was measured with a pressure transducer (Model PX 105, Omega Engineering, Stamford, CT). Mixing in the reservoir was induced with a magnetic stirrer. The reservoir was sealed to avoid gas exchange with the atmosphere and a check valve was mounted on the reservoir vent. The membrane module was oriented horizontally.

The static or gassing out method was employed to measure the hydrogen transfer coefficient in the sealed-end membrane module. Hydrogen transfer occurred as water was pumped through the shell side of the module resulting in an increase in dissolved hydrogen concentration in the reservoir with time. Dissolved hydrogen concentration was measured with an Orbisphere Micro Logger (Model 3654, Orbisphere Laboratories, Neuchatel, Switzerland) in 15-second intervals for the duration of 0.5 hours. Water temperature and atmospheric pressure were recorded for each test. The effect of water

flow rate on the hydrogen mass transfer coefficient was investigated. Experiments were completed with various pumping speeds in the range of 0.2 L/min to 0.6 L/min while hydrogen gas pressure on the inside of hollow fibers was held constant. The effect of gas pressure on the hydrogen mass transfer coefficient was investigated by holding the water flow rate constant and varying hydrogen pressure in the range from 1 psig to 4 psig.

The experimental configuration shown in Figure 4.4 was employed to obtain a correlation of the hydrogen mass transfer coefficient with flow characteristics. In this method, hydrogen gas was first sparged into the 2.5-L closed mixed reservoir to raise the dissolved hydrogen concentration. Hydrogenated water was recirculated through a flow-through membrane module by a peristaltic pump (Model 7553-70, Cole-Parmer, Vernon Hills, IL). An air purge flowed through the lumen of the horizontally oriented hollow fibers at approximately 1L/min with an aid of a peristaltic pump of the above model. Hydrogen was stripped from the liquid phase into the gas phase resulting in decrease of hydrogen concentration with time in the closed vessel. The dissolved hydrogen concentration was measured with the Orbisphere Micro Logger over time.

Physical membrane module parameters manipulated in the flow-through study were (1) shell diameter and (2) length of fiber. The characteristics of the membrane modules tested are summarized in Table 4.1.

## 4.4 Data Analysis

In a microporous hollow fiber, the driving force for hydrogen transfer is provided by the hydrogen concentration gradient between the gas and the liquid phase across the

membrane. Hydrogen transfer through hollow fiber membranes occurs by the mechanism of Knudsen diffusion with the concentration gradient as a driving force. The hydrogen transfer involves three sequential steps, as shown in Figure 4.5. First, the hydrogen molecules diffuse out of the bulk air phase to the membrane surface, second, they diffuse through the gas filled pores in the walls of the hydrophobic hollow fibers. Finally, when the hydrogen molecules reach the other side of the membrane, they diffuse into the water phase. The mass transfer coefficient (K), or resistance to mass transfer (1/K), is given by

$$\frac{1}{K} = \frac{1}{k_L} + \frac{1}{k_m H} + \frac{1}{k_G H} \tag{4.1}$$

where $k_L$, $k_m$, and $k_G$ are the individual mass transfer coefficients in the liquid, across the gas filled membrane pores and in the gas phase, respectively (cm/s); H is the dimensionless Henry's law constant.

Gas diffusion coefficients are approximately four orders of magnitude greater than diffusion coefficients in water. Since both $k_G$ and $k_m$ are characterized by gas phase diffusivities, they are expected to be much larger in value than $k_L$. In addition hydrogen is only slightly soluble in water (i..e., the value of H is large). It follows that the resistances $\frac{1}{Hk_G}$ and $\frac{1}{Hk_m}$ are expected to be negligible compared to $\frac{1}{k_L}$. Therefore, hydrogen transfer is limited by liquid film diffusion in the membrane system.

### 4.4.1 Sealed-end Configuration

For steady state operation when gas is transferred from the gas phase to the liquid phase, the hydrogen gas flux, N, across the membrane can be written as

$$N = Ka\left(C^* - C_L\right) \tag{4.2}$$

where $N$ is hydrogen flux (mg/cm$^2$-s); $K$ is the overall hydrogen mass transfer coefficient (cm/s); $a$ is the specific surface area (cm$^2$/cm$^3$); $C^*$ is the water phase hydrogen concentration in equilibrium with the gas phase (mg/L); and $C_L$ is the hydrogen concentration in the liquid phase at any position along the module (mg/L). In a membrane system, the value of 'a', the specific surface area, can be calculated from the surface area of the fibers.

Hydrogen transfer across a single fiber can be described by:

$$v_L \frac{dC_L}{dz} = Ka\left(C^* - C_L\right) \tag{4.3}$$

where $v_L$ is the water velocity through the hollow fiber module(cm/s) and $z$ is the position along the length of the membrane module (cm).

If the hydrogen pressure equals the regulated feed pressure everywhere within the fiber, then $C^*$ is constant. If the influent dissolved hydrogen concentration, $C_1$, is a constant, then the boundary conditions $C_L=C_1$ at $z=0$ and $C_L=C_2$ at $z=L$ apply, where $C_2$ is the liquid phase hydrogen concentration in the module outlet stream and L is the length of the module. Integration of equation 4.3 then yields:

$$C_2 = C^* - (C^* - C_1)\exp\left(-\frac{KaL}{v_L}\right) \tag{4.4}$$

The water from the module was recirculated back to the reservoir where the hydrogen concentration change was measured with time. The hydrogen component mass balance around the well-mixed reservoir in Figure 4.6 is:

$$V\frac{dC_1}{dt} = QC_2 - QC_1 \tag{4.5}$$

where $Q$ is the water flow rate (L/sec) and $V$ is the volume of the reservoir (L).

Substituting $C_2$ from equation 4.4 and rearranging gives:

$$\ln\left(\frac{C^* - C_L}{C^*}\right) = \frac{Q}{V}\left[1 - \exp\left(-\frac{KaL}{v_L}\right)\right]t \tag{4.6}$$

Consequently, the mass transfer coefficient may be obtained form the slope of the graph of $\ln\left(\frac{C^* - C_L}{C^*}\right)$ vs. time.

### 4.4.2 Flow-through Configuration

In flow-through studies, hydrogen was transferred from the liquid phase to the gas phase. This particular case is governed by the following flux equation:

$$N = -Ka\,(C_L - C^*) \tag{4.7}$$

Since the membrane lumen is constantly replenished by fresh air, the gas phase hydrogen concentration C* is equal to zero. In this case, equation 4.7 becomes

$$N = -Ka\,C_L \tag{4.8}$$

Dissolved hydrogen concentration gradient along the length of the membrane module results from hydrogen flux:

$$N = -Ka\ C_L = v_L \frac{dC_L}{dz} \tag{4.9}$$

If the influent dissolved hydrogen concentration, $C_1$, is a constant, then the boundary conditions $C_L=C_1$ at $z=0$ and $C_L=C_2$ at $z=L$ apply. Integration of equation 4.9 then yields:

$$C_2 = C_1 \exp\left(-\frac{KaL}{v_L}\right) \tag{4.10}$$

Substituting $C_2$ from equation 4.10 into the mass balance around the well-mixed reservoir in equation 4.5 and rearranging gives:

$$\frac{dC_1}{C_1} = \frac{Q}{V}\left[\exp\left(-\frac{KaL}{v_L}\right) - 1\right]dt \tag{4.11}$$

This equation is subject to the following boundary conditions:

$$t = 0, \qquad C_1 = C_0$$

$$t = t, \qquad C_1 = C$$

Integrating, we obtain the following exponential equation:

$$\ln\left(\frac{C}{C_0}\right) = \frac{Q}{V}\left[\exp\left(-\frac{KaL}{v_L}\right) - 1\right]t \tag{4.12}$$

Therefore, the overall mass transfer coefficient can be determined from the slope of $\ln(C/C_0)$ time plot.

There are two important assumptions in the above development:

(a) the experiment was always conducted in such a way that the residence time in the reservoir was large compared to the response time of the hydrogen sensor;

(b) the concentration of hydrogen in the reservoir changes slowly compared to the concentration changes occurring in the module for the assumption of steady state in the module to be realistic.

## 4.5 Results and Discussion

Laboratory scale experiments were conducted to evaluate the influence of operating conditions on the performance of the sealed-end hollow fiber module. A typical result is shown in Figure 4.7. The data were plotted in the form of equation 4.6. The mass transfer coefficient was obtained from the slope of each plot. Hydrogen mass transfer coefficient was found to increase with water flow rate. Figure 4.8 provides a comparison between experimental values of the mass transfer coefficient at various water flow rates. This trend was also observed in oxygen transfer results in similar configurations (Ahmed and Semmens, 1992). Sell *et al.* (1993) also report a linear relationship between hydrogen flux and water flow rate in the laminar flow regime. Hydrogen mass transfer coefficient values for each variable pressure run are also shown in Figure 4.8. The apparent pressure dependence may be related to nitrogen and oxygen counter diffusion through the membrane pores. A correction for counter diffusion of dissolved gases is needed to account for the phenomenon. Both water flow rate and

hydrogen gas pressure increased the hydrogen mass transfer coefficient which ranged form 0.000115 cm-$s^{-1}$ to 0.00282 cm-$s^{-1}$. The values of mass transfer coefficient (K) obtained with hollow fiber modules are several orders of magnitude greater than the corresponding values for bubble aeration .

In each of the flow-through tests, the reservoir concentration data also generated a linear relationship when plotted in the form of Equation 4.12. A typical plot of ln ($C/C_o$) versus time is provided in Figure 4.9. The overall mass transfer coefficient can be extracted from the slope of the line using experimental operating conditions and module parameters.

In order to normalize the data, it is convenient to express the parameters in terms of the dimensionless Sherwood Number (Sh), Reynolds Number (Re), and Schmidt Number (Sc) as follows:

$$Sh = \alpha \, Re^{\beta} \, Sc^{\gamma} \qquad (4.13)$$

where $\alpha$, $\beta$, and $\gamma$ are constants. The definitions of dimensionless numbers are presented in Table 4.2. The Schmidt number is defined as the ratio of the kinematic viscosity of a fluid to the diffusivity of the solute in that fluid. Since hydrogen was the only constituent considered in this study and test temperature only varied within a few degrees, the Schmidt number may considered to be constant, and a 1/3 power dependence was assumed from literature (Bennett and Myers, 1982).

When fluid flow in conduits (in this case hollow fibers) is considered, it is also necessary to determine a "characteristic length" term for Reynolds number calculations.

The characteristic length is defined as the effective diameter, $d_e$ (cm) (Yang and Cussler, 1986):

$$d_e = \frac{4(\text{cross-sectional area of flow})}{\text{wetted perimeter}} \tag{4.14}$$

The experimental data were plotted as Sherwood number versus Reynolds number in Figure 4.10. A least squares regression analysis of the data gave the following correlation:

$$Sh = 0.0027\ Re^{1.44}$$

$$\text{or,} \qquad Sh = 0.00043\ Re^{1.44}\ Sc^{0.33} \tag{4.9}$$

The plot shown in Figure 4.10 shows a significant amount of scatter ($R^2$ = 0.69); however, the relationship is significant at the 95% confidence level. Yang and Cussler (1986) found that the use of the ratio $d_e/L$ to modify Reynolds number improved the correlation with the Sherwood number. The experimental data thus were plotted as Sherwood number versus $Red_e/L$ in Figure 4.11 to obtain the following correlation:

$$Sh = 16.77\ (Red_e/L)^{1.02}$$

$$\text{or,} \qquad Sh = 2.68\ (Red_e/L)^{1.02}\ Sc^{0.33} \tag{4.10}$$

The modified correlation was successful in reducing the scatter ($R^2$ = 0.83) in the hydrogen transfer data collected in this study. The exponent of the term (Rede/L) was also comparable to that reported for oxygen transfer (Yang and Cussler, 1986).

The mass transfer correlation developed in this work is compared in Table 4.3 with those found in the literature. The mass transfer correlation indicates the results of this study are very similar to those expected for flow in small tubes. However, the

coefficient in front of the present mass transfer correlation is large; about an order of magnitude greater than the values reported by other researchers (Yang and Cussler 1986; Ahmed and Semmens, 1992) for similar hollow fiber membrane systems.

## 4.6 Conclusions

A membrane process for transferring hydrogen gas to water was studied using microporous membranes. The membrane is hollow fiber microporous polypropylene, and hydrophobic to prevent wetting of membrane pores by water. The hydrogen transfer is primarily controlled by liquid film diffusion. The values mass transfer coefficient (K) obtained with hollow fiber modules are several orders of magnitude greater than the corresponding values for bubble aeration. The following mass transfer correlation can be used to design membrane modules for hydrogen transport:

$$Sh = 2.68\ (Red_e/L)^{1.02}\ Sc^{0.33}$$

The membrane hydrogen transfer appears to be a viable technology for transferring hydrogen gas to water. Further investigation is required to evaluate large-scale applications and other operating concerns.

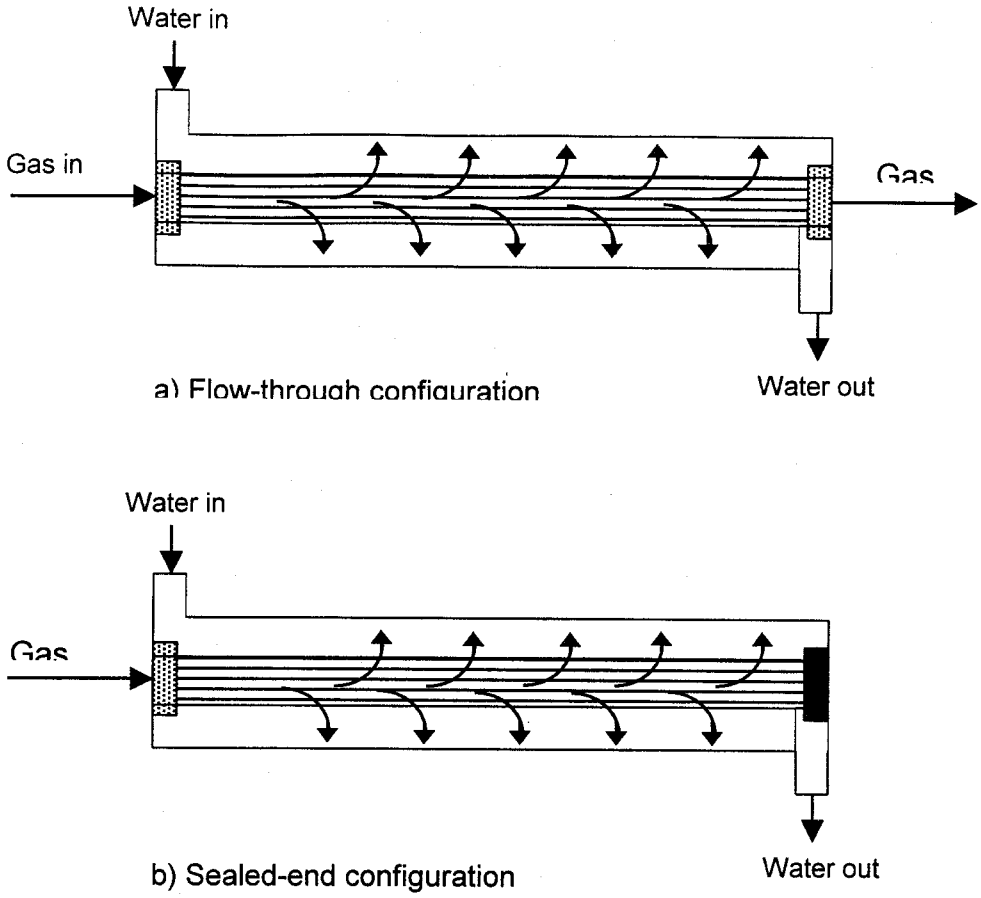


**Figure 4.1: Flow-through and sealed-end modules**

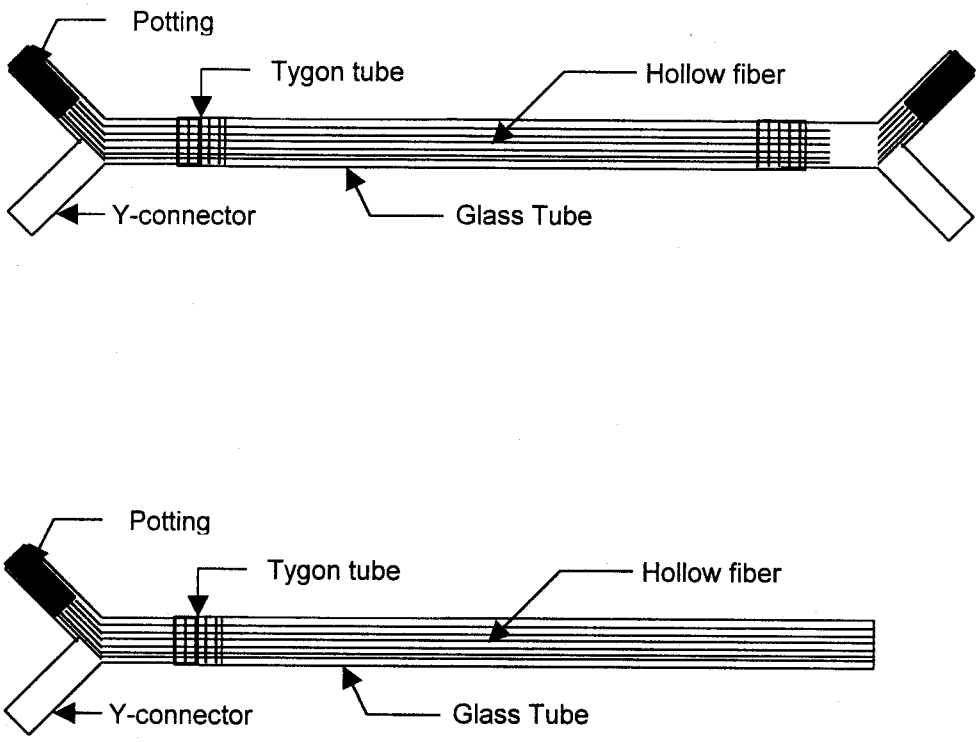


**Figure 4.2: Schematic diagram of membrane modules**

**Table 4.1: Dimensions of hollow fiber membrane modules**

| No. of Fibers | Fiber Diameter (cm) | Length (cm) | Equivalent Diameter (cm) | Shell Diameter (cm) |
|---|---|---|---|---|
| 36 | 0.03 | 125 | 0.195 | 0.6 |
| 6 | 0.03 | 69 | 0.454 | 0.6 |
| 1 | 0.03 | 80 | 0.57 | 0.6 |
| 1 | 0.03 | 71 | 0.37 | 0.4 |
| 6 | 0.03 | 63.5 | 0.266 | 0.4 |

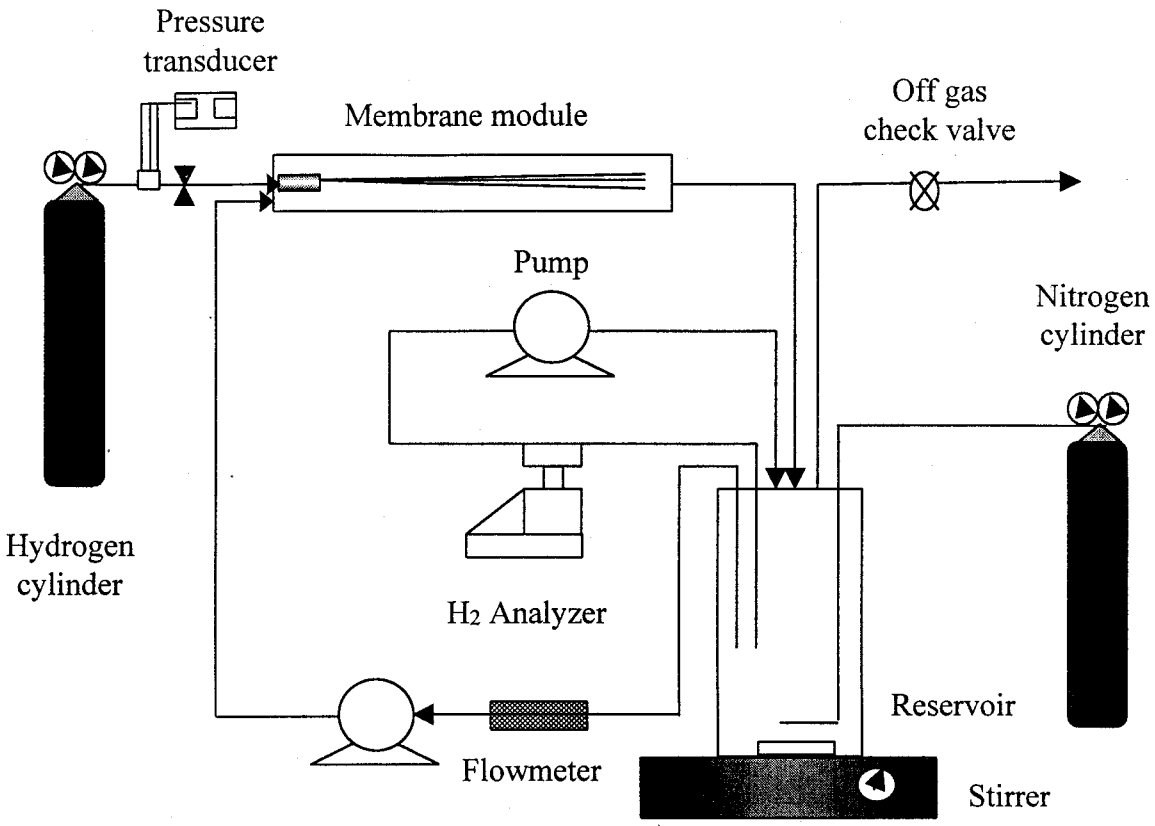


**Figure 4.3: Sealed-end hydrogen transfer experimental set-up**

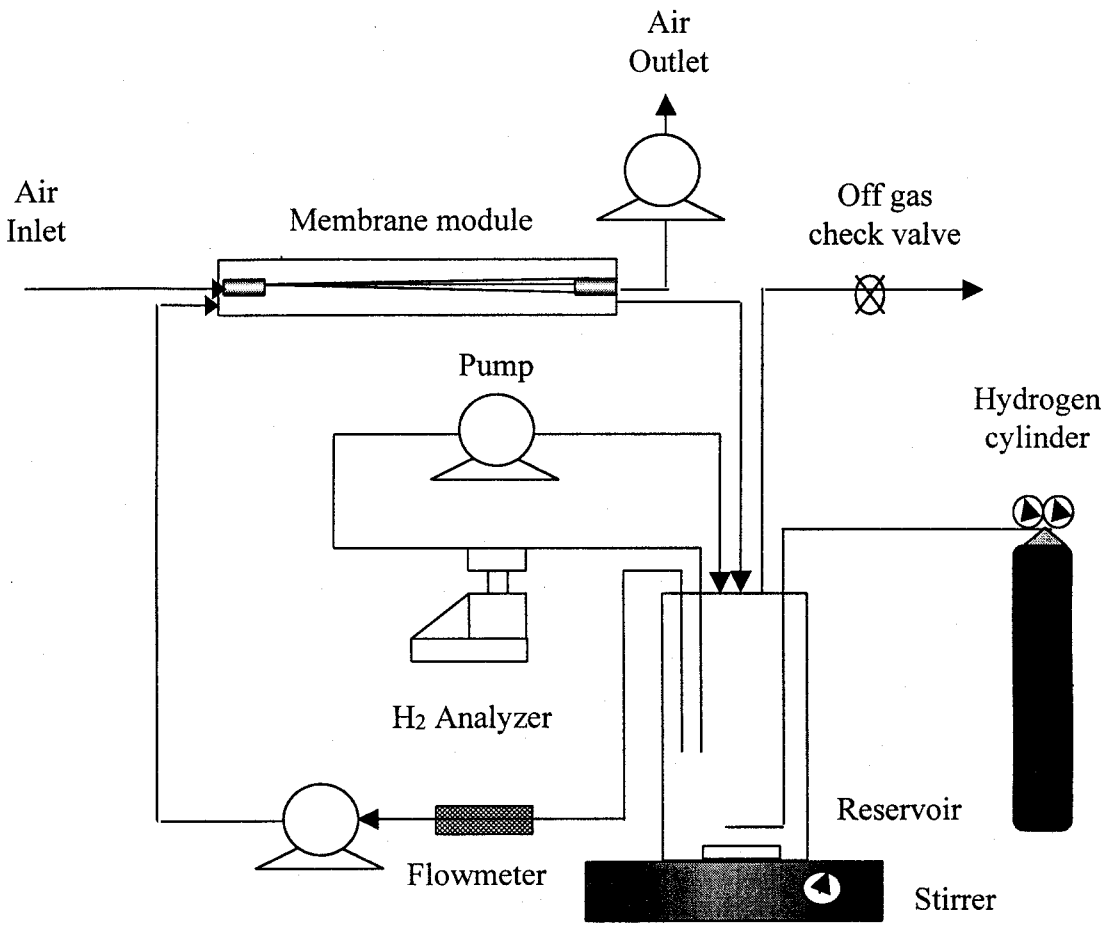


**Figure 4.4: Flow-through hydrogen transfer experimental set-up**

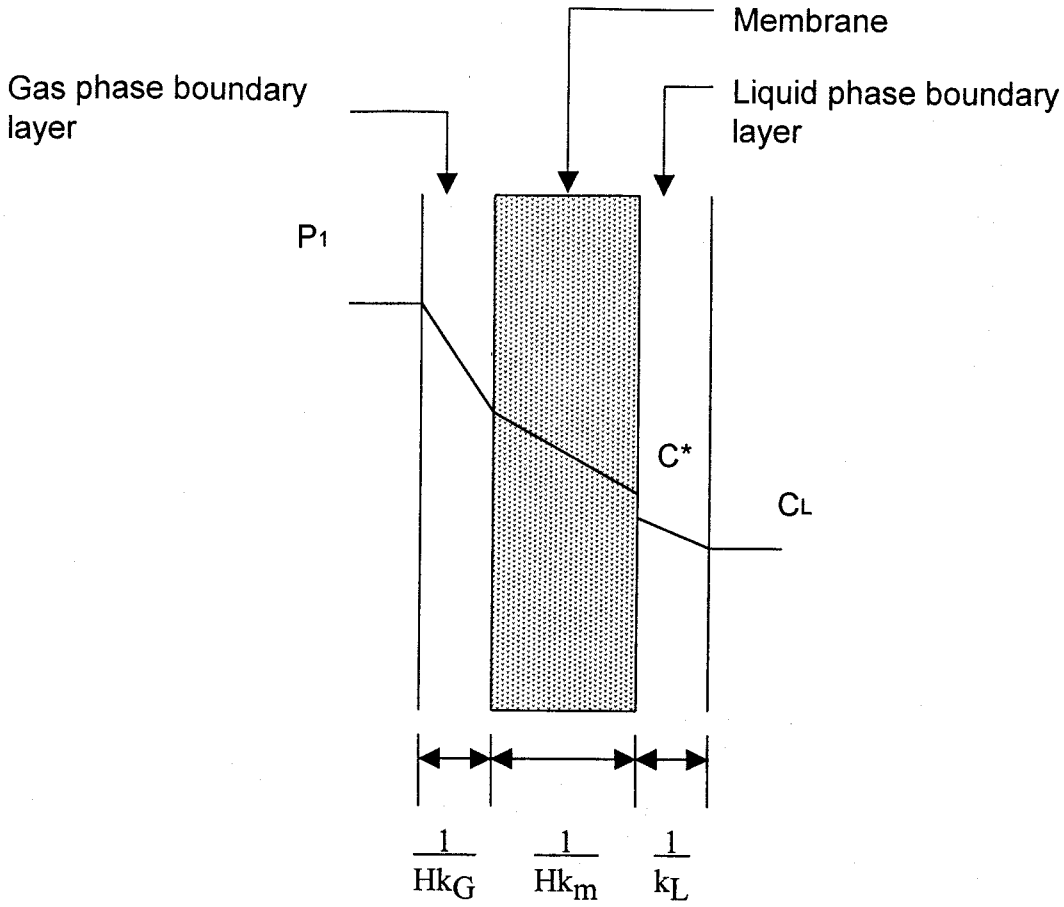


**Figure 4.5: Resistance contribution to gas transfer across a membrane wall.**

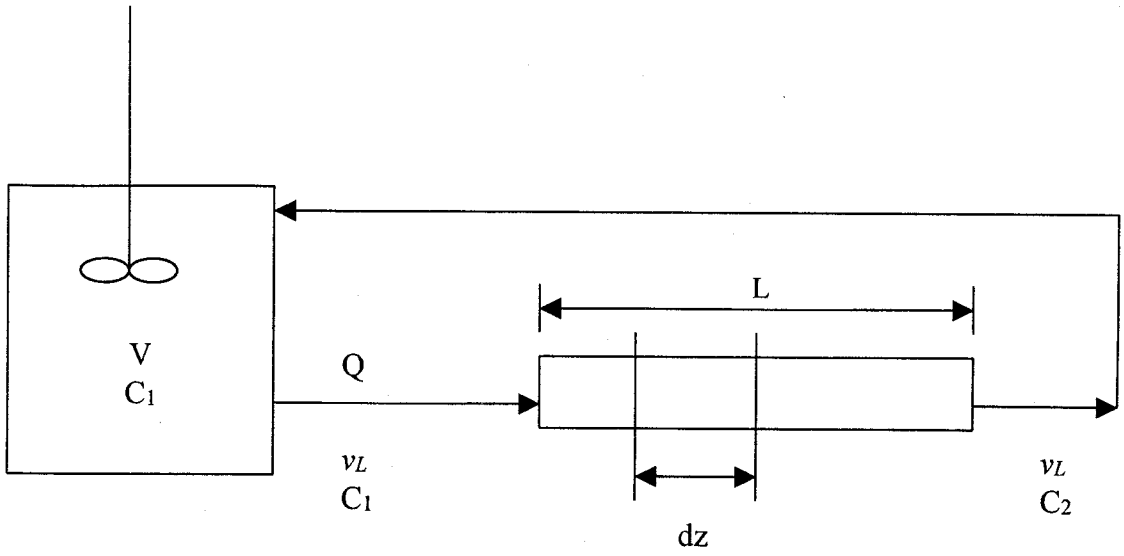


**Figure 4.6: Hydrogen transfer modeling diagram**

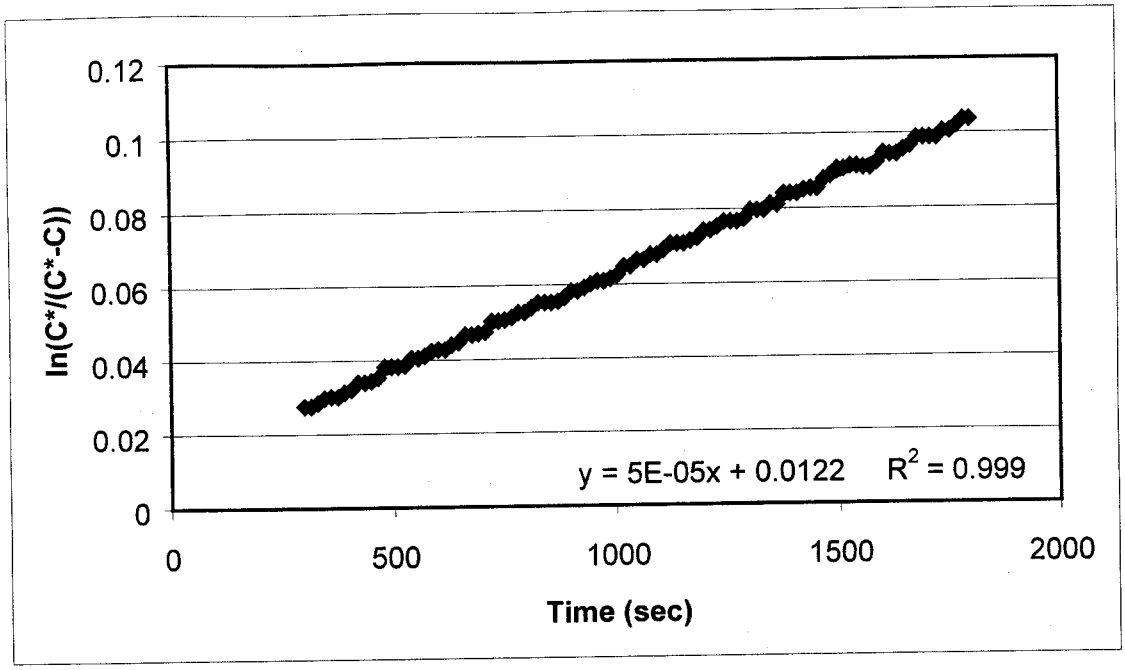


**Figure 4.7: Sample ln(C*/(C*-C) versus time plot for sealed-end configuration**

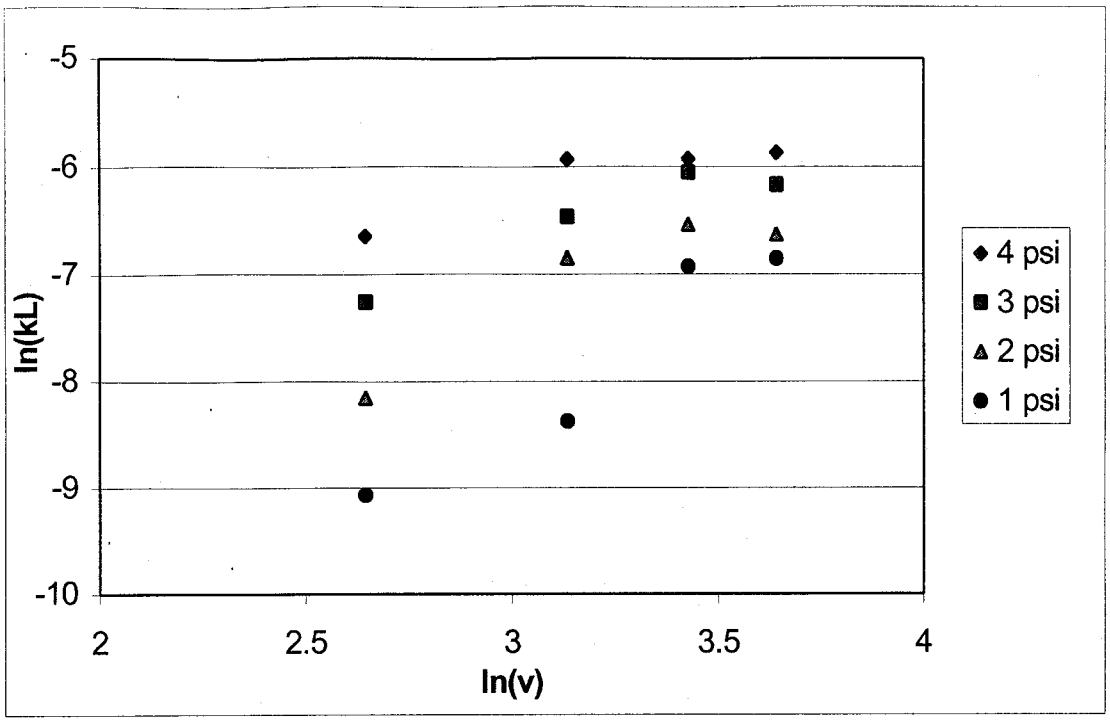


**Figure 4.8: Influence of water velocity and hydrogen pressure on the mass transfer coefficient in sealed-end configuration**

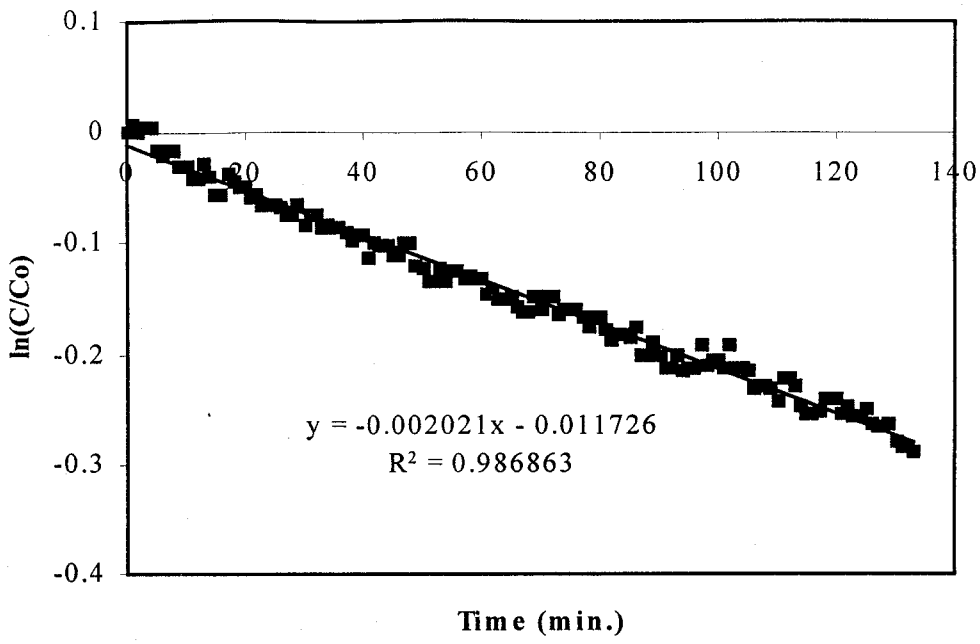


**Figure 4.9: Sample ln(C/Co) versus time plot for flow-through configuration**

**Table 4.2: Definition of the dimensionless numbers in mass transfer**

| Name | Symbol | Definition |
|---|---|---|
| Reynold's number | Re | $\frac{d_e v_L}{\nu}$ |
| Schmidt number | Sc | $\frac{\nu}{D}$ |
| Sherwood number | Sh | $\frac{d_e k_L}{D}$ |

Where $d_e$ is equivalent diameter (cm); $v_L$ is water velocity (cm/s); $\nu$ is kinematic viscosity (cm2/s); $D$ is hydrogen diffusivity in water (cm2/s); $k_L$ is the mass transfer coefficient (cm/s)

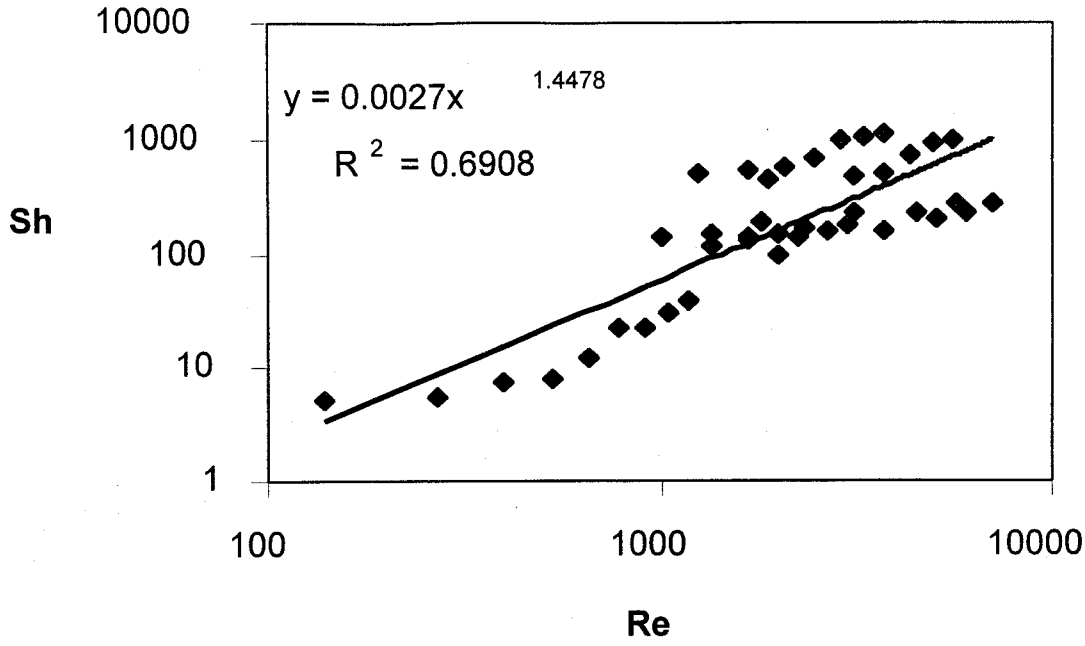


**Figure 4.10: Mass transfer correlation for designing hollow fiber membrane modules (Sh vs. Re)**

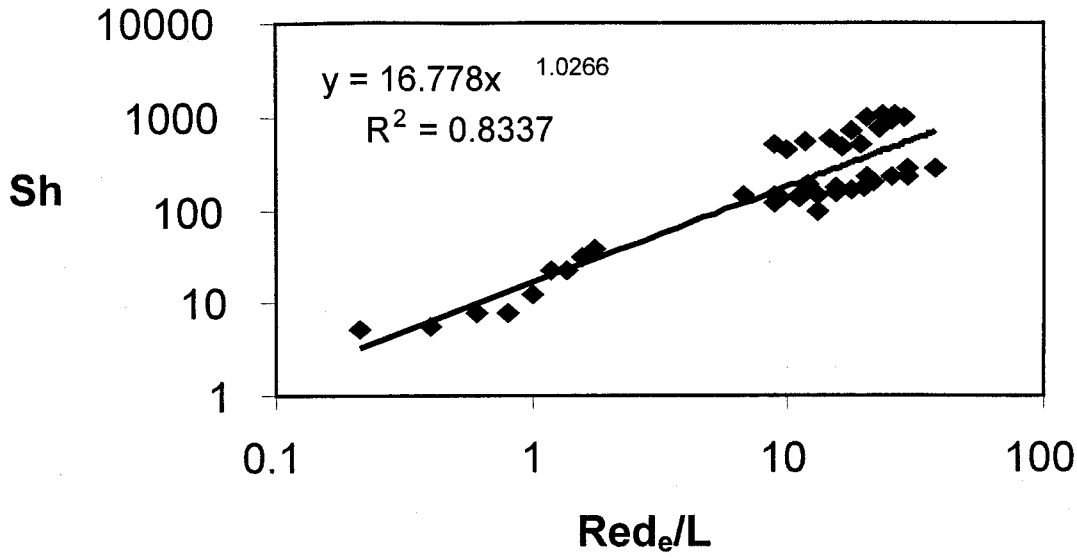


**Figure 4.11: Mass transfer correlation for designing hollow fiber membrane modules (Sh vs. Red$_e$/L)**

**Table 4.3: Comparison of correlations from transfer literature**

| Reference | Correlation | Re Range |
|---|---|---|
| Knudsen and Katz (1958) | $Sh = 0.022\ Re^{0.6}\ Sc^{0.33}$ | |
| Yang and Cussler (1986) | $Sh = 1.25\ (Red_e/L)^{0.93}\ Sc^{0.33}$ | 5 - 3000 |
| Cote et al. (1989) | $Sh = 0.61\ Re^{0.363}\ Sc^{0.33}$ | 0.6 - 49 |
| Ahmed and Semmens (1992) | $Sh = 0.108\ Re^{0.81}\ Sc^{0.33}$ | 300 - 46000 |
| | $Sh = 0.886\ (Red_e/L)^{0.91}\ Sc^{0.33}$ | |
| This Study | $Sh = 0.00043\ Re^{1.44}\ Sc^{0.33}$ | 350 - 4200 |
| | $Sh = 2.68\ (Red_e/L)^{1.02}\ Sc^{0.33}$ | |

# CHAPTER 5

# CONTINUOUS FLOW FIXED FILM REACTOR STUDIES

## 5.1 Introduction

One of the main objectives of this study was to evaluate the performance of denitrifying autotrophic hydrogen oxidizing bacteria in a bench-scale reactor with a gas delivery membrane system. An upflow fixed-film reactor was constructed and operated in the laboratory to evaluate the feasibility of supplying hydrogen via a membrane module. The reactor was inoculated with hydrogen oxidizing bacteria and operated in batch mode until a stable biofilm was developed on the media. In continuous flow mode an anoxic inorganic nutrient buffer solution containing 22.6 mg/L $NO_3^-$-N was fed to the reactors at varying hydraulic retention times.

## 5.2 Materials and Methods

### 5.2.1 Fixed-bed Bioreactor

The fixed bed reactor consisted of a cylindrical clear acrylic column, 2.54 cm in diameter and 14 cm in height. The top and the bottom of the reactor were fitted with rubber stoppers. Tygon tubing was connected to a hole in each stopper. The schematic of the reactor is shown in Figure 5.1. Polymeric rings were used as reactor media (Figure 5.2). Previous studies demonstrated that the performance of the polymeric rings medium

was found to be superior in hydrogenotrophic denitrification to other investigated media in the range of 2 to 8 hours retention times (Benedict *et al.* , 1998). The effective area available for biofilm growth was 0.0697 $m^2$.

The reactor packing was coated with an acclimated biofilm at column start-up. A mixed culture was obtained from the anoxic denitrification basin of the Winslow Wastewater Treatment Plant (Winslow, NJ). An acclimated culture for autotrophic denitrification was developed in batch reactors at room temperature. The column was connected to a stirred vessel which contained 2L of a degassed inorganic nutrient buffer solution containing 100 mg/L nitrate and 100 mg/L sodium carbonate to which 83.3 mL of acclimated culture seed was added. Hydrogen gas was sparged into the stirred vessel in 5 second pulses at 2 hour intervals. The liquor was withdrawn from the tank and recycled through the column using a peristaltic pump (Model 755-70, Cole-Parmer, Vernon Hills, IL) at a flow rate of 220 mL/min. Periodically, the vessel was purged with hydrogen to maintain the dissolved oxygen concentration below 1 mg/L. pH was maintained at 7.0 with carbon dioxide gas addition. The schematic of the apparatus used for start-up is provided in Figure 5.3.

### 5.2.2 Hollow Fiber Membrane Module

Hollow fiber membrane module construction and materials has been described in Section 4.4. A schematic of a sealed-end module has been presented earlier in Figure 4.2.

### 5.2.3 Continuous Operation

Continuous flow studies were conducted using carbonate as sole inorganic carbon source and sodium nitrate as the electron acceptor for the autotrophic denitrification culture. Sodium carbonate ($Na_2CO_3$), sodium nitrate ($NaNO_3$), phosphate buffer ($KH_2PO_4$ and $K_2HPO_4$) and micronutrients ($MgSO_4 \cdot 7H_2O$, $CaCl_2$, and $FeSO_4 \cdot 7H_2O$) were obtained from Sigma Chemicals Co. (St. Louis, MO). High purity hydrogen and carbon dioxide gas were obtained from MG Gas Industries (Malvern, PA). Deionized distilled water from a Barnstead Water Purification Water System (Dubuque, IA) was used for preparation of all solutions.

The experimental set-up for the flow through studies is shown in Figure 5.5. Influent entered the system from a feed tank kept under hydrogen and was continuously recycled between the two stages by a peristaltic pump (Model 7553-70, Cole-Parmer, Vernon Hills, IL). Effluent was withdrawn from the top the fixed-bed bioreactor by a cassette pump (Sarah Standard Cassette Pump, Manostat Corporation, Barrington, IL). The system operating parameters are listed in Table 5.1.

The reactor was operated in continuous mode by supplying a degassed inorganic feed buffer solution using the Sarah cassette pump. Hydrogen gas was delivered through a 6 fiber sealed end hollow fiber module. The system was closed to the atmosphere, with the excess gas being expelled using check valves at the feed water reservoir.

### 5.2.4 Analytical Methods

The following parameters were monitored during the course of the continuous experiments:

- pH,
- Alkalinity,
- Nitrate and Nitrite, and
- TOC (Total Organic Carbon) and DOC (Dissolved Organic Carbon).

Nitrate and nitrite were measured using the Standard Method 4500-B (AWWA *et al.*, 1995) and HACH Method 8153, on a spectrophotometer (Model HACH DR 4000U, Loveland, CO.), respectively. An Orion 720 pH Meter was used to measure the effluent pH. Alkalinity was determined using a HACH digital titrator according to Standard Method 2130 B (Standard Methods 1995; 2130 B). Dissolved oxygen concentrations were measured with a DO Meter (Model YSI 520, YSI, Inc., Yellow Springs, CO). TOC and DOC concentrations were determined using the HACH Method 10324 on a spectrophotometer (Model HACH DR 4000U, Loveland, CO)

## 5.3 Results and Discussion

During operation, the membrane surface appeared to be clean; there was no visible biofilm growth on the membrane surface. The influent was buffered adequately, therefore, no pH shift was observed in the effluent as shown in Figure 5.6. The alkalinity of the reactor effluent was consistently higher (by about 130 mg/L) than the influent under steady state operation (Figure 5.7). This is expected since alkalinity is generated

during the biological nitrate reduction process. Ergas and Reuss (2001) and Lee and Rittmann (2000) reported similar increases in alkalinity. Effluent TOC was measured to be 8.2 mg/L and dissolved organic carbon was 5.7 mg/L for 0.2 L/min recycle flow rate. The dissolved organic carbon concentration exceeded the level of 2.3 mg/L reported in literature for a hollow fiber membrane bioreactor (Lee and Rittmann, 2000). This behavior may be due to a higher biomass concentration in the reactor and high water velocity, contributing to shearing of the biofilm. Therefore, effluent organic carbon concentration may be decreased with further optimization of biofilm thickness and recycle flow rate.

The effluent nitrate and nitrite concentrations are presented in Figure 5.8 as a function of time. At an HRT (hydraulic retention time) of 10 hours, complete nitrate removal was observed during steady state condition. Nitrite effluent concentration was 1mg/L of $NO_2$-N complying with drinking water standard. The overall nitrate and nitrogen removal efficiencies were 100% and 95%, respectively. The recycle rate was set at 0.2 L/min to control biofilm growth on the membrane surface.

The hydrogen pressure in the membrane module was held at 6 psi. Using the membrane module parameters and mass transfer correlation developed earlier in Chapter 4, the hydrogen transfer rate of the membrane module at 6 psi operating pressure, was estimated to be $1.31 \times 10^{-3}$ mg/sec. From reaction stoichiometry, the hydrogen requirement corresponding the reactor nitrate loadings was estimated to be $1.31 \times 10^{-5}$ mg/sec. Therefore, it is evident that the hydrogen transfer rates were about two order of magnitude (100 times) greater than the stoichiometric hydrogen requirement and the process is not expected to be hydrogen limited at this loading condition.

The reactor was also operated at 6.75, 3.25 and 1.75 hour HRTs by increasing the influent flow rate. The hydrogen pressure in the membrane module was reduced to 1 psi due to frequent hydrogen bubbling problems. The steady state pH, alkalinity, nitrogen species and percentage removals for 6.75, 3.25 and 1.75 hour HRT are presented in Figures 5.5 through Figure 5.9. After about 130 hours of operation, at 6.75 hr HRT, the influent tank was found to have visible growth of slime layers on the inside of the reservoir surface. The influent nitrate concentration also dropped as a result of this contamination as shown in Table 5.3. The influent tank and the tubing were replaced with cleaned and autoclaved tank and tubing, however, no change in reactor performance was observed. No other significant operating problems were encountered during the experiments. The reactor operation was discontinued with the appearance of 1.27 mg/L of $NO_3$-N at 1.75-hour HRT time and subsequent decrease of removal efficiencies as shown in Figure 5.19 and Figure 5.20, respectively. The ratio of hydrogen delivered to stoichiometric hydrogen requirement rate was about 5. Therefore, one of the factors that may be limiting at 1.75-hr HRT was dissolved hydrogen concentration. It should be noted, however, that increasing the following physical and operating parameters would increase the hydrogen transfer rate from the membrane module:

- length of the fiber and the module,
- number of fibers,
- diameter of the fibers,
- recycle flowrate through the module, and
- operating pressure.

Table 5.2 also shows no nitrate and low constant nitrite concentrations in the reactor effluent for 10, 6.75 and 3.25 detention times; this may be an indication that the concentrations of dissolved hydrogen in the reactor were not limiting for the HRTs. Efforts were made to measure the dissolved hydrogen concentration in the reactor effluent by connecting the effluent line to the Orbisphere hydrogen sensor. The dissolved hydrogen concentration varied from 30 to 40 ppb at 1 psi operating pressure. Effluent dissolved hydrogen concentration was not measured at 6 psi operating pressure.

The steady state volumetric $NO_3$-N loading rate and removal efficiencies per unit surface area for each detention time was calculated and presented in Table 5.3Hydraulic retention time reported is an empty bed value obtained by dividing the volume of reactor column by the influent flow rate. The corrected hydraulic retention time ($HRT_a$) was calculated as follows:

$$HRT_a = (V_{HFM} + V_r - V_m)/Q_{in} \qquad (5.1)$$

where $HRT_a$ = hydraulic detention time, hours

$V_{HFM}$ = Volume of water in the module, liters

$V_r$ = Volume of reactor column, liters

$V_m$ = Volume of media, liters

$Q_{in}$ = Influent flow rate, liters/hr

The membrane module volume was used in calculating hydraulic detention time because the recycle ratios were sufficiently high, so the entire system could be considered a complete mix flow reactor (CMFR).

The results show that the optimum performance with low (about 0.68 mg/L) nitrite concentration would be achieved between 1.75 and 3.25-hr detention time. The

reported loading rates and the corresponding effluent concentrations may be used for scale up purposes for similar systems. The reactor performance was compared with other similar studies in the literature and is presented in Table 5.4. The surface area removal efficency of 13.2 $mg/m^2$-h is lower than reported for other attached growth processes which ranged from 33 $mg/m^2$-h to 104 $mg/m^2$-h. However, the volumetric removal rate of 0.312 kg $NO_3$-$N/m^3$-day is in the range of other studies (0.059 kg $NO_3$-$N/m^3$-3.95 kg $NO_3$-$N/m^3$). Both results may be increased by raising the hydraulic retention time at higher hydrogen transfer rates.

The recycle ratios where determined by dividing the flow into the reactor by the recycle flow rate through the membrane reactor and are presented in Table 5.5. Recycle ratio may be an operational concern since it is much higher than those recommended for trickling filters (Metcalf and Eddy, 1991). Recycle rates provide control of oxygen transfer rates and biofilm thickness on the media in typical trickling filter operations. Higher recycle rate would result in higher pumping requirements, thereby increasing the operating cost. However, the recycle ratios were found to be within the range of similar studies employing autotrophic denitrification reactors.

## 5.4 Conclusions

A stable biofilm was developed in the packed bed reactor that removed nitrate using hydrogen as the electron donor. Hydrogen gas was successfully delivered to the reactor via the hollow fiber membrane gas transfer module. The calculated hydrogen

transfer rate of the given module indicated that the system did not experience hydrogen limitations up to a HRT of about 3.25 hours.

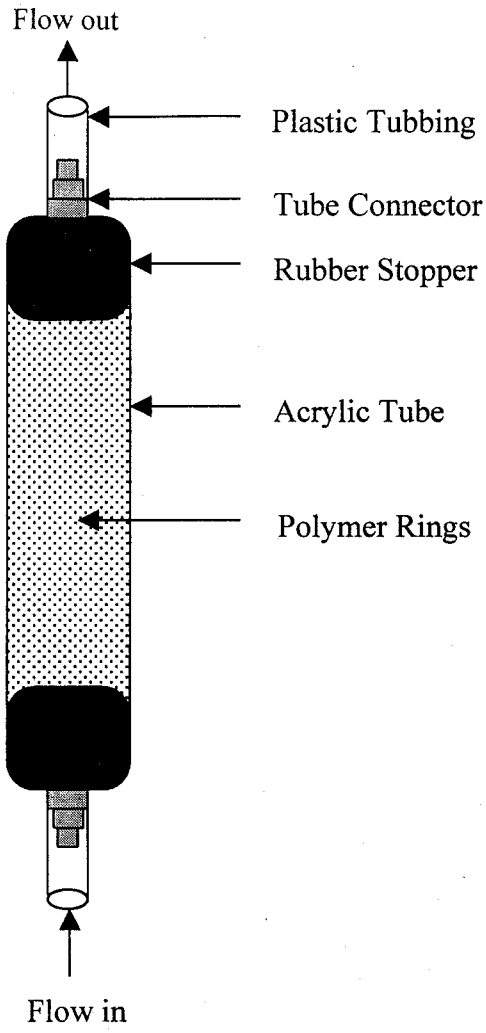


**Figure 5.1: Schematic of the fixed biofilm reactor**

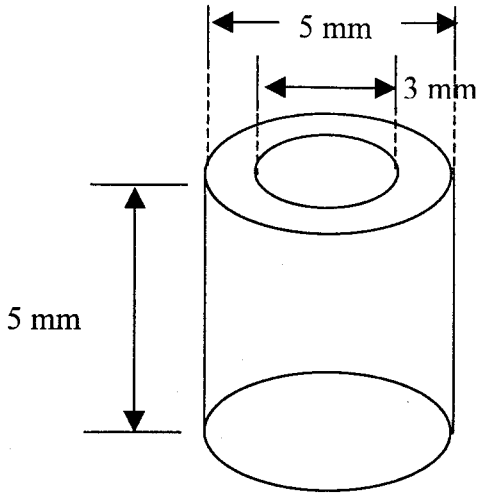


**Figure 5.2: Polymeric reactor media**

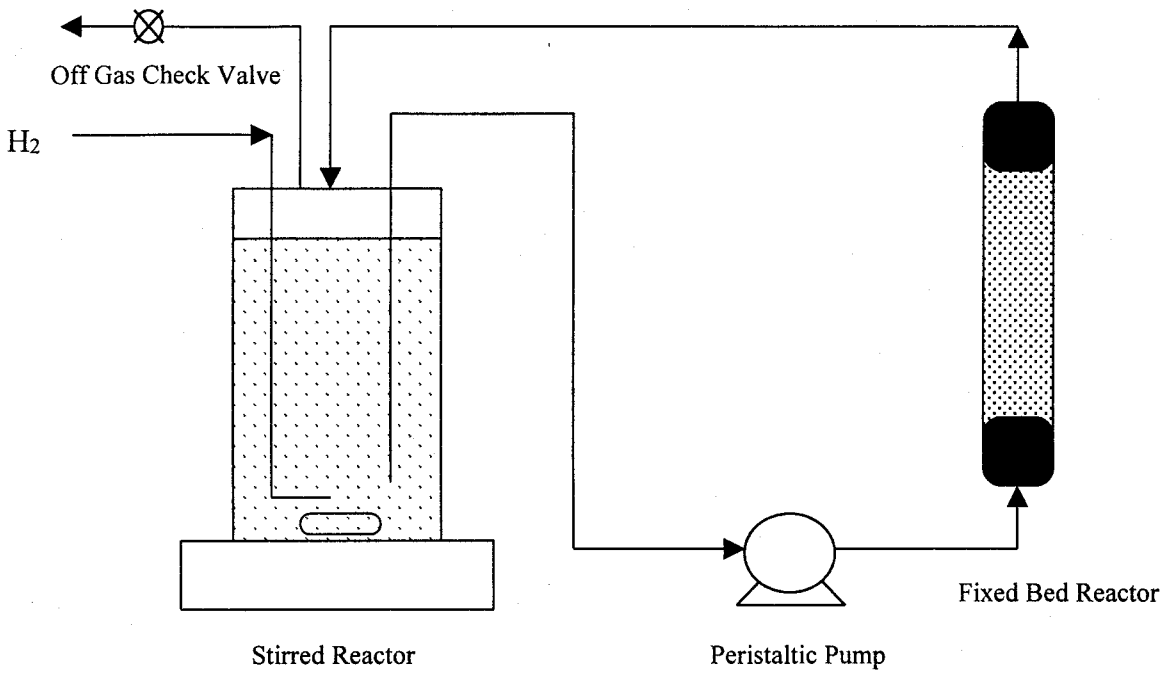


**Figure 5.3: Fixed biofilm reactor start-up configuration**

**Table 5.1: Continuous-flow fixed film reactor parameters**

| | |
|---|---|
| Influent flowrate (mL/min) | 0.1-0.7 |
| Influent pH | 6.57 |
| Influent alkalinity (mg/L as $CaCO_3$) | 400 |
| Hydrogen gas pressure (psig) | 6 |
| Recycle flow rate (L/min) | 0.1-0.2 |
| | |
| **Influent composition** | **Concentration (mg/L)** |
| $NaNO_3$ | 100 |
| $NaCO_3$ | 100 |
| $K_2HPO_4$ | 1,190 |
| $K_2HPO_4$ | 980 |
| $MgSO_4 \cdot 7H_20$ | 100 |
| $CaCl_2$ | 30 |
| $FeSO_4 \cdot 7H_2O$ | 3.75 |

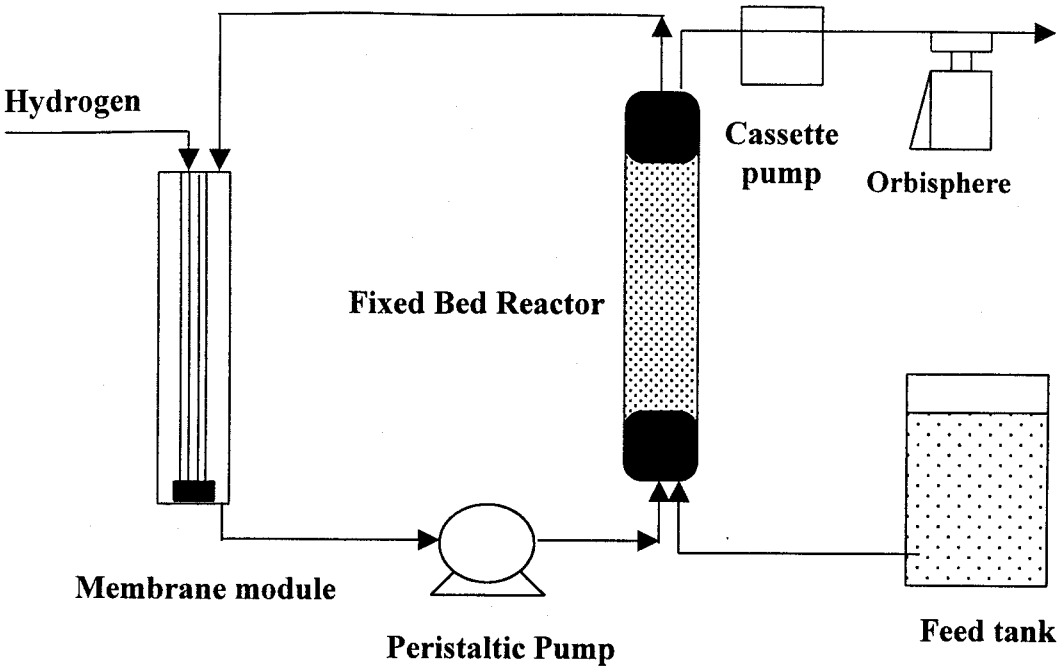


**Figure 5.4: Continuous flow fixed film reactor set-up**

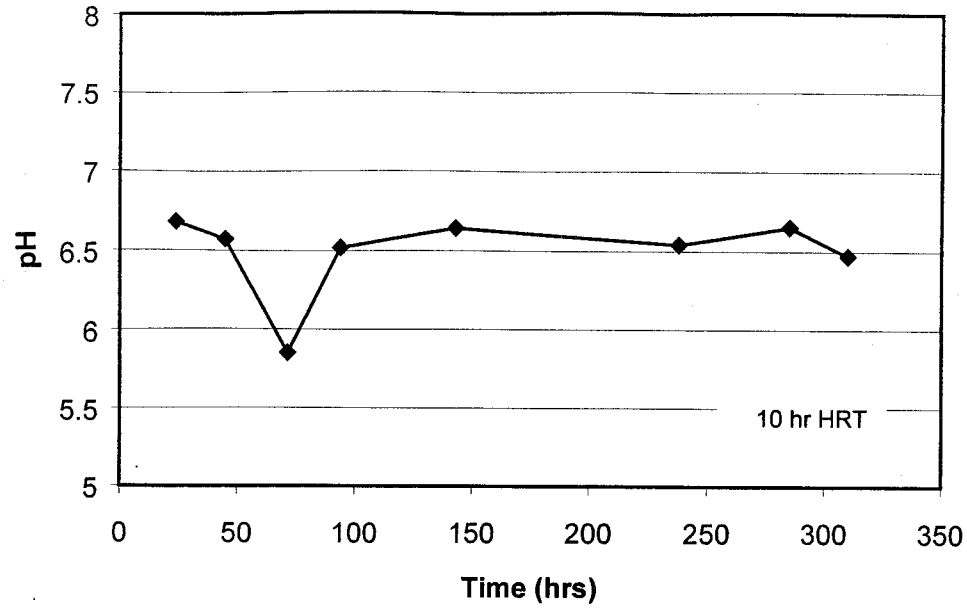


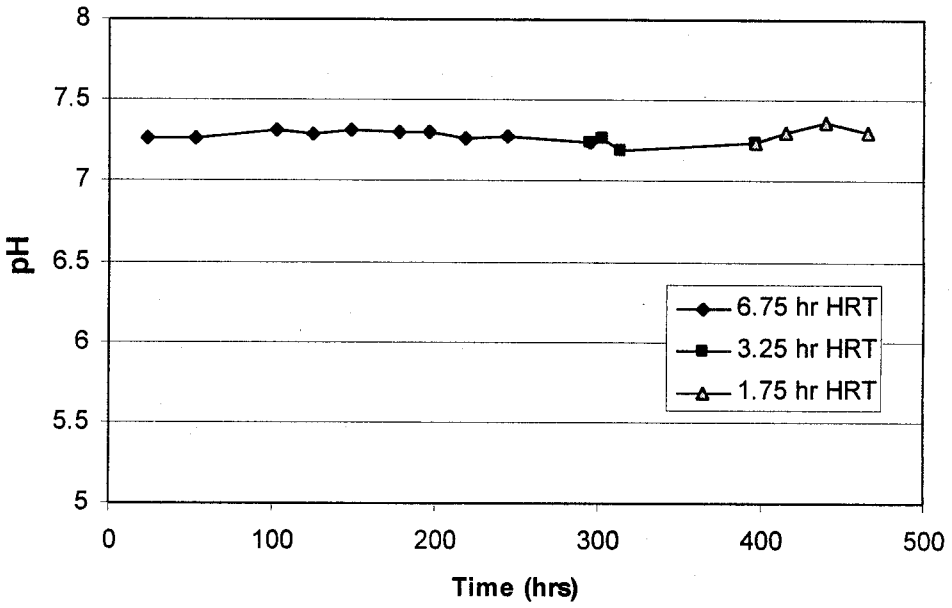


**Figure 5.5: Reactor effluent pH with time**

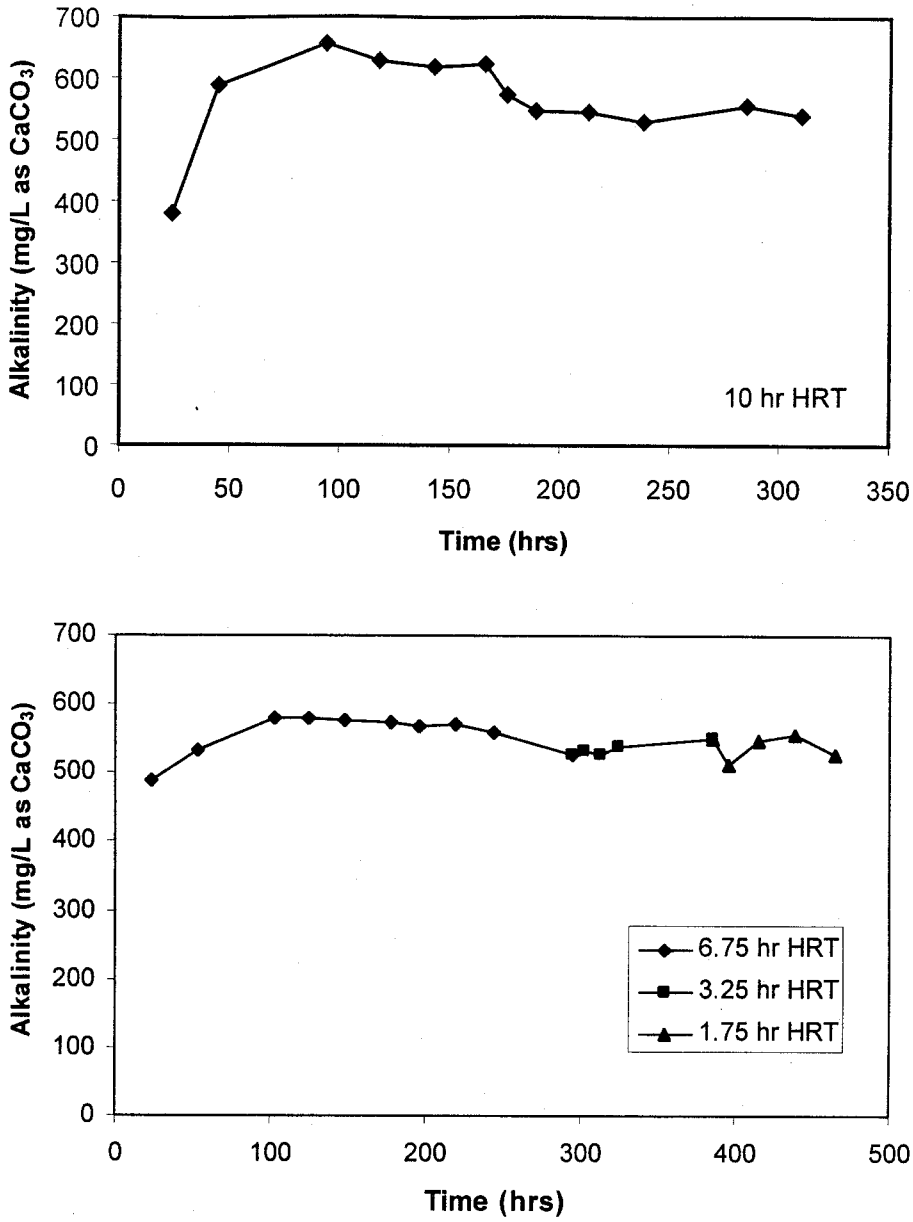


**Figure 5.6: Effluent alkalinity as a function of time**

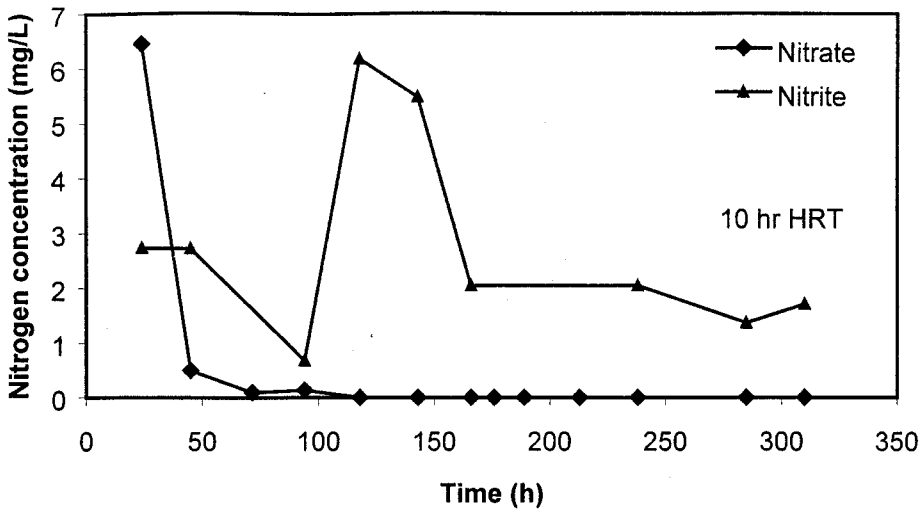


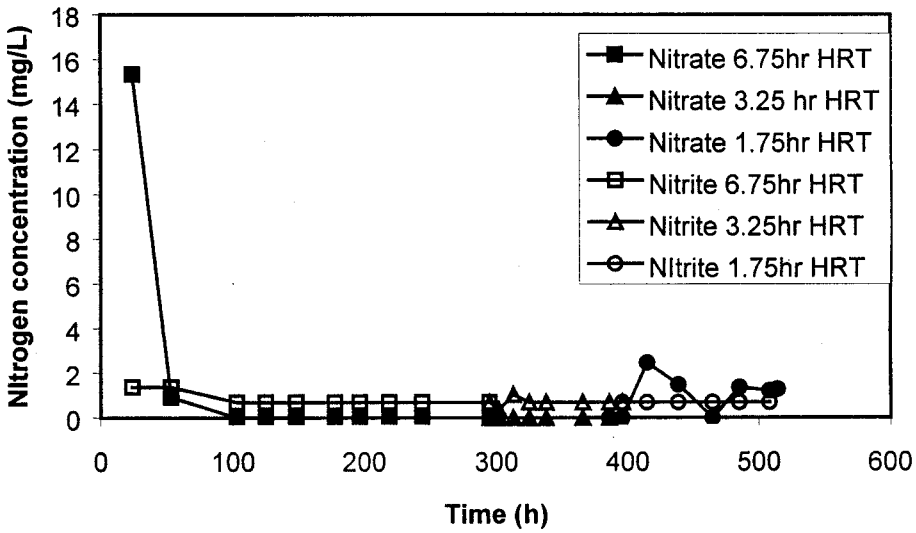


**Figure 5.7: Effluent nitrate and nitrite concentration with time**

**Table 5.2: Overall steady state performance of fixed-film continuous flow membrane bioreactor**

| HRT (hr) | Influent | Effluent | | | | | % Removal | |
|---|---|---|---|---|---|---|---|---|
| | $NO_3$-N (mg/L) | pH | Alkalinity (mg/L as $CaCO_3$) | $NO_3$-N (mg/L) | $NO_2$-N (mg/L) | Total-N (mg/L) | $NO_3$-N | Total-N |
| 10 | 22.6* | 6.5 | 556 | 0 | 1.54 | 1.54 | 100 | 93.1 |
| 6.75 | 20.46 | 7.2 | 565 | 0 | 0.68 | 0.68 | 100 | 96.67 |
| 3.25 | 16.64 | 7.2 | 552 | 0 | 0.68 | 0.68 | 100 | 95.8 |
| 1.75 | 13.58 | 7.3 | 528 | 1.27 | 0.68 | 1.95 | 90.6 | 85.5 |

*Calculated

**Table 5.3: Continuous-flow fixed film reactor steady state results**

| $HRT_a$ (hr) | HRT (hr) | Volumetric loading mg $NO_3$-N /$m^3$-h | Surface area removal efficiency mg $NO_3$-N /$m^2$-h | Effluent nitrate concentration mg $NO_3$-N/L | Effluent nitrite concentration mg $NO_2$-N/L |
|---|---|---|---|---|---|
| 0.5 | 1.75 | 12,978 | 13.21 | 1.5 | 0.67 |
| 1 | 3.25 | 6,906 | 7.03 | 0 | 0.67 |
| 2 | 6.75 | 3,335 | 3.40 | 0 | 0.67 |
| 3 | 10 | 2,263 | 2.30 | 0 | 1 |

**Table 5.4: Continuous-flow fixed film reactor performance**

| | % Removal | HRT (hr) | Surface area removal efficiency (mg $NO_3$-N/ $m^2$-h) | Volumetric removal rate (kg $NO_3$-N/ $m^3$-day) |
|---|---|---|---|---|
| Benedict et al. (1996) | | 6 | 42.7 | 2.63 |
| Lee and Rittmann (2000) | 76, 92 | 0.7 | 33, 42 | 2.6, 3.95 |
| Ergas and Reuss (2001) | 90 | 30 | 104 | 0.059 |
| This study | 93 | 1.75 | 13.2 | 0.312 |

**Table 5.5: Recycle Ratio Comparison**

| | System Configuration | Recycle Ratio |
|---|---|---|
| Metcaff and Eddy (1991) | Trickling Filters | 0.5-2 |
| Lee and Rittmann (2000) | Hollow Fiber Membrane Bioreactor | 175 |
| Ergas and Reuss (2001) | Hollow Fiber Membrane Bioreactor | 125-755 |
| Benedict et al. (1996) | Fixed film Bioreactor | 114-343 |
| This study | Fixed Film Bioreactor | 143-500 |

# CHAPTER 6

# CONCLUSIONS AND RECOMMENDATIONS

The main goal of this research was to evaluate the feasibility of a continuous flow fixed film bioreactor coupled with a hollow fiber membrane module for autotrophic denitrification. Kinetic coefficients for autotrophic denitrifying bacteria were obtained from batch studies. Design relationships for hydrogen gas transfer using hollow fiber membranes were developed. Finally, the effect of detention time and hydrogen transfer on nitrate removal in the system was evaluated.

Results of this study enabled a number of conclusions to be drawn and revealed areas for further investigation.

## 6.1 Conclusions

The following conclusions can be made from this study:

1. Autorophic denitrifying hydrogen oxidizing bacteria are easily isolated from seed bacteria obtained from a biological denitrification facility.
2. The following kinetic coefficients were obtained: $\mu_m$ of 0.65 $d^{-1}$, Y of 0.78 mg cells/mg $NO_3$-N, and $k_d$ of 0.04 $d^{-1}$.
3. Hydrogen gas delivery via hollow fiber membranes is feasible for attached growth processes.

4. Hydrogen-to-water transfer through sealed-end hollow fiber membranes is dependent on hydrogen gas pressure and water flow rate.

5. The following mass transfer correlation can be used to design membrane modules for hydrogen dissolution into water:

$$Sh = 2.68\ Red_e/L^{1.02}Sc^{0.33}$$

6. Increasing the concentration of dissolved hydrogen through application of hollow fiber membranes ensured nitrate limited biofilm and eliminated explosive conditions from accumulation of hydrogen gas in headspaces.

7. A 3.25 hour hydraulic retention time was needed to successfully reduce 22.4 mg/L $NO_3$-N to nitrate and nitrite concentrations below drinking water standards.

8. No significant nitrite accumulation was observed during system operation. Effluent nitrite concentrations met the maximum contamination level of 1mg $NO_2$-N/L.

9. Increased levels of TOC and DOC indicate that additional treatment is needed following the denitrification process since elevated organic concentrations may result in bacterial growth in the distribution system.

## 6.2 Recommendations for Future Studies

Two areas of possible future study were identified: (1) long-term sealed-end membrane module operation for hydrogen delivery, (2) optimization of biofilm thickness.

Counter-diffusion of other gas species dissolved in water impacts membrane module operation. Back diffusion of nitrogen and oxygen from the water into the fiber has a significant effect on the hydrogen partial pressure along the fiber causing an apparent pressure dependence of the measured mass transfer coefficients. A gas-phase composition model is required to analyze the impact of nitrogen and oxygen on operation of hollow fiber membranes for hydrogen transfer. Long term operation may also result in flooding of membrane fibers with water over time. Effective flushing procedures are required for system maintenance.

The biofilm thickness should be optimized as a function of recycle rate. Biofilm thickness varies with flow rate of fluid through the fixed bed bioreactor. In the two-stage system this parameter corresponds to the recycle rate. As the recycle rate is increased, more cells will shear off the surface of the biofilm. A thin biofilm may not provide an adequate cell mass to carry out denitrification with a desired rate. However, an overly thick biofilm may cause substrate depletion at the surface of the plastic media resulting in sloughing. Since hydrogen transfer rate also depends on the system recycle rate, optimization must take into account the constraints necessary for gas transfer. Of major concern is biological fouling caused by biofilm growth on the membranes in prolonged operation. Increased recycle flow rate is expected to shear accumulated biofilm off the membrane surface. Cleaning methods are needed for long term operation of the gas transfer modules.

In the future, biological processes may show potential for hydrogen delivery in autotrophic denitrification. Kubota Corporation, Japan is developing a process for hydrogen production that makes use of genetically engineered photosynthetic bacteria

(Kubota, 2002). The microorganisms also use industrial or organic wastewater as a substrate. Potentially, a photosynthetic reactor may be placed upstream of the autotrophic denitrification reactor to hydrogenate water. Simultaneously, the photosynthetic bacteria can remove organic contamination present in the water stream. In this manner, the hydrogen requirement may be satisfied with no outstanding operating costs. Thus, nitrate removal with hydrogen oxidizing bacteria may be expected to make a favorable impact on water treatment.

## REFERENCES


Ahmed, T., and Semmens, M. J. (1992a) Use of sealed end hollow fibers for bubbleless membrane aeration: experimental studies. , *J. Membr. Sci.*. **69**,1-10.

Ahmed, T., and Semmens, M. J. (1992b) The use of independently sealed microporous hollow fiber membranes for bubbleless oxygenation of water: model development, *J. Membr. Sci.*, **69**,11-20.

Albertson, O. E., and Davis, G. (1984) Analysis of process factors controlling performance of plastic bio-media, presented at the *57th Annual Meeting of the Water Pollution Control Federation*, New Orleans, LA.

American Water Works Association (AWWA), 1995, Surveys reveal pesticides, nitrates in water from farming areas, *J. - Am. Water Works Assoc.*, **87**(10), 13-14.

Barrenstein, A.; Kramer, U.; and Obermann, P. (1986) Underground treatment of nitrate rich groundwater by infiltration with treated wastewater or methane-rich natural gas, *DVGW-Schriftenreihe*, Wasser, **106**, 99-116.

Benedict, S. W. (1996) Denitrification with autotrophic hydrogen oxidizing bacteria, *M.S. Thesis*, University of Nevada, Reno.

Benedict, S.W.; T. Ahmed; and K. Jahan (1996) Autotrophic denitrification using hydrogen oxidizing bacteria in continuous flow biofilm reactor. *Toxicol. Environ. Chem.*, **67**, 197-214.

Bennett, C.O., and Myers, J.E. (1982) *Momentum, Heat and Mass Transfer*, Third Edition, McGraw-Hill, New York.

Brautigam, H. J., and J. Sekoulov. (1987) Dentrification with hydrogen as an electron donor introduced through nonporous membranes. *Ber. Abwassertech. Ver.* **37**, 555-65.

Brezonik, P.L. (1977) Denitrification in Natural Waters, *Prog. Wat. Tech.*, **8**(4-5),373-392.

Brindle, K.; Stephenson, T.; and Semmens, M.J. (1998) Nitrification and oxygen utilization in a membrane aeration bioreactor. *J. Membr. Sci.*, **144**, 197.

Chang, C. C.; Tseng, S. K.; and Huang, H. K. (1999) Hydrogenotrophic denitrification with immobilized *Alcogenes eutrophus* for drinking water treatment. *Bioresour. Technol.*, **69**, 53-58.

Claus, G., and Kutzner, H. J. (1985) Autotrophic Denitrification Thiobacillus denitrificans, *Appl. Microbiol. Biotechnol.*, **22**, 289-296.

Clifford, D., and Liu, X. (1993) Ion Exchange for Nitrate Removal, *J. - Am. Water Works Assoc.*, **85**(4),135-143.

Cote, P.L.; Bersillon, J.; and Huyard, A. (1989) Bubble-Free Aeration Using Membranes: Mass Transfer Analysis, *J. Membr. Sci.*, **47**, 91 - 106.

Croll, B. T. (1985) Biological fluidized-bed denitrification for potable water. *Advances in Water Engineering, Proc.International Symposium*, T. H. Y. Tebbut, ed. Elsevier Appl. Sci., London, 180-187.

Croll, B.T., and Hayes, C. R. (1988) Nitrate and water supplies in the United Kingdom, *Envir. Pollut. (Oxford, UK)*, **50**,163-187.

Delanghe, B.; Nakamura, H.; Myoga, H.; and Magara, Y. (1994a) Biological Denitrification with ethanol in a membrane bioreactor, *Environ. Technol.*, **15**, 61-70.

Delanghe, B.; Nakamura, J.; Myoga, H.; Magara, Y.; and E. Guibal (1994b) Drinking water Denitrification in a Membrane Bioreactor, *Water Sci. Technol.*, **30** (6) 157-160.

Dries, D.; Liessens, J.; Verstrate, W.; Stevens, P.; Vos, P. de; and Ley, J. (1988) Nitrate removal from drinking water by means of hydrogenotrophic denitrifiers in a polyurethane carrier reactor. *Water Supply*, **6**, 181-192.

Eckenfelder, W. W., Jr.( 1963) Trickling filter design and performance, *Trans. ASCE*, **128**.

Eckenfelder, W. W., Jr. (1989) *Industrial Water Pollution Control*, 2nd ed., McGraw-Hill, New York.

Ergas, S. J., and Reuss, A.F. (2001) Hydrogenotrophic denitrification of drinking water using a hollow fibre membrane bioreactor. *J. Water Supply: Res. Technol.--AQUA* **50**(3), 161-171.

Flere, J. M., and T. C. Zhang (1998) Remediation of nitrate contaminated surface water using sulfur and limestone autotrophic denitrification. *Water Resour. Urban Environ.--98, Proc. Natl. Conf. Environ. Eng.*

Freeze, R. A., and Cherry, J. A., *Groundwater*, Prentice Hall, Englewood Cliffs, N. J., 1979.

Fuchs, W.; Schatzymayr, G.; and Braun, R. (1997) Nitrate removal from drinking water using a membrane-fixed biofilm reactor. *Appl. Microbial Biotechnol.*, **48**, 267-274.

Gantzer, C.J. (1995) Membrane dissolution of hydrogen for biological nitrate removal. *Proc. Water Environ. Fed. 68th Annu. Tech. Exposition Conf.*, Miami Beach, Florida, pp. 49-60.

Gaudy, A.R., and Gaudy, E.T., (1988) *Elements of Bioenvironmental Engineering*, Engineering Press, Inc., San Jose, CA.

Gayle, B.P.; G.D. Boardman; J.H. Sherrard; and R.E. Benoit (1989) Biological denitrification of water, *J. Environ.l Eng.*, **115**(5), 930-943.

Germain, J. E. (1966) Economic treatment of domestic waste by plastic media trickling filter, *Journal WPCF*, **38**, 2.

Ginocchio, J. (1983) Process and apparatus for the denitrification of groundwater, *European Patent Appl., EP 86863 Al*, Aug. 31.

Godart, H., and Gonnard, P. (1991) Co-current denitration on resin: three years practical experience. *International Water Services Association Copenhagen Congress*. Special Subject No. 1.

Gross, H., and Treutler, K. (1986), Biological denitrification process with hydrogen oxidizing bacteria for drinking water treatment, *Aqua*, **5**, 288-290.

Gross, H.; Schnoor. G.; and Ruther, P. (1988) Biological denitrification process with hydrogen oxidizing bacteria for drinking water treatment, *Water Supply*, **6**,193.

Hallberg, G. R. (1989) Nitrate in ground water in the United States, in Nitrogen Management and Ground Water Protection, *Developments in Agriculture and Managed-Forest Ecology*, Elsevier, New York.

Ho, C.M.; S.K. Tseng; and Y.J. Chang (2001) Autotrophic denitrification via a novel membrane-attached biofilm reactor. *Letters in Applied Microbiology*, **33**, 201-205.

Hoerner, G., and A. Irmer (1989) Autotrophic biological denitrification with the membrane fluidized-bed technology with hydrogen as electron donor. *Vom Wasser* **73,** 429-47.

Ishida, H., and Imashiro, A. (2001) Biological nitrogen removal method and device. *Jpn. Kokai Tokkyo Koho*. 20

Islam, S., and Suidan, M. T. (1994) Enhancement and control of denitrification using a biofilm electrode reactor. *Proc. Water Environ. Fed. Tech. Exposition Conf,,* Chicago, IL, pp 217-225.

Iversen, S. (1995) Absorption or stripping using hollow-fiber membranes. (FLS Miljoe A/S, Den.). *PCT Int. Appl.*, **83**.

Jiang, W.; Qu, J.; Lei, P.; Liu, S.; and Meng, G. (2001) Nitrate nitrogen removal from groundwater by autotrophic denitrification in a packed bed reactor. *Zhongguo Huanjing Kexue*, 2**1**(2), 133-136.

Jimenez, K.M.; Zander, A.K.; and S.J. Grimberg (1998) Membrane enhanced biofilm reactor for treatemnt of high Strenght Wasatewaters Containing Nitrophenilic Compounds. *Proc. Water Environ. Fed. 71st Annu. Tech. Exposition Conf* Orlando, Fl.

Kapoor, A., and Viraraghavan, T., 1997, Nitrate removal from drinking water – Review, *J.Environ. Eng.g*, **123**, 371-380.

Keskiner, Y., and S. J. Ergas (2000) Hollow fiber bioreactor for aqueous and gas phase ammonia removal by nitrification. *Proceedings of the Mid-Atlantic Industrial and Hazardous Waste Conference.* Lancaster, PA: Technomic Pub. Co., 867-876.

Kim, E.-W., and Bae, J.-H. (2000) Alkalinity requirements and the possibility of simultaneous heterotrophic denitrification during sulfur utilizing autotrophic denitrification. *Water Sci. Technol*, 42(3-4, Water Quality Management in Asia), 233-238.

Knudsen, J.G., and Katz, D.L. (1958) *Fluid Dymamics and Heat Transfer*, McGraw-Hill, New York.

Korom, S. (1992) Natural denitrification in the saturated zone: A review, *Water Res.*, **28**(6), 1657-1668.

Kuai, L., and Verstraete, W. (1999) Autotrophic denitrification with elemental sulphur in small-scale wastewater treatment facilities. *Environ. Technol,* **20**(2), 201-209.

Kubota Corporation, New Energy and Industrial Development Organization, Advanced Technology Laboratory (2002) http://www.kubota.co.jp/english/tecno/advanced.html

Kurt, M.; Dunn, J.; and Bourne, J. R. (1987), Biological denitrification of drinking water using autotrophic organisms with hydrogen in a fluidized-bed reactor. *Biotechnol. Bioeng.*, **29**,493-501.

Lazarova, V.Z.; Capdeville, B; and Nikolov, L. (1992) Biofilm Performance of a Fluidized Bed Biofilm Reactor for Drinking Water Denitrification, *Water Sci. Technol.*, **26**(3-4), 555-566.

Lee, K-C., and Rittmann, B.E. (2000) A novel hollow-fibre membrane biofilm reactor for autohydrogenotrophic denitrification of drinking water. *Water Sci.d Technol.*, **14**(4-5), 219-226.

Li, K. ; Kong, J. ; and Tan, X. (2000) Design of hollow fibre membrane modules for soluble gas removal. *Chem. Eng. Sc.,*. **55**(23),5579-88.

Liessens, J.; Germonpre, R.; Beernaert, S.; and Verstrate, W. ( 1993a) Removing nitrate with a methylotrophic fluidized bed: technology and operating performance, *J. - Am. Water Works Assoc.*, **85**(4), 144-154.

Liessens, J.; Germonpre, R.; Kersters, I.; Beernaert, S.; and Verstrate, W. ( 1993b) Removing nitrate with a methylotrophic fluidized bed: microbiological quality *J. - Am. Water Works Assoc.*, **85**(4), 155-161.

Lowry, O. H.;.Rosebrough, N. J; Farr, A.L.; and Randall, R.J. (1951) Protein measurements with the folin phenol reagent, *J. Biol. Chem.* **193**, 265-275.

Mateju, V.; Cizinska, S. ; Kreici, J.; and Janoch, T.( 1992) Biological water denitrification – a review. *Enzyme Microbial Technology.* **14**, 170-183.

Metcalf and Eddy, Inc. (1991) *Wastewater Engineering: Treatment, Disposal, and Reuse*, McGraw Hill, 3rd edition, New York, NY.

Miki, S., and Kato, T. (2001) Nitrogen removal from wastewater by biological denitrification using autotrophic bacteria. *Jpn. Kokai Tokkyo Koho*, 6.

Miyake, Y.; Myoga, H.; and Magara, Y. (1997) Several factors affecting the specific denitrification rate of hydrogen oxidizing bacteria. *Water Use Conserv., Mex. '96 Workshop.*

Novak, P.J., Edstrom, J.A., Clapp, L.W., Hozalski, R.M. and Semmens, M.J. (2001) Stimulation of dechlorination by membrane delivered hydrogen: Small Field Demonstration, Proceedings of the 6th International Symposium on In-Situ and On-site Bioremediation, San Diego, CA.

Oh, S.-E; Kim, K.-S.; Choi, H.-C.; Cho, J.; and Kim, I. S. (2000) Kinetics and physiological characteristics of autotrophic denitrification by denitrifying sulfur bacteria. *Water Sci. Technol.* **42**(3-4)

Pekdemir, T.; Kacmazoglu, E.K.; Keskilner, B.; and Algur, O.F. (1998) Drinking water denitrification in a fixed bed packed biofilm reactor. *Turkish Journal of Engineering and Environmental Sciences*, **22**, 39-45.

Peyton, B.M. (1994) *100 area groundwater biodenitrification bench-scale treatability study – Final Report, WHC-SD-EN-ES-043.* Westinghouse Hanford Company, Richland, WA.

Peyton, B.M.; Mormille, M.R.; and Petersen, J.N. (2001) Nitrate reduction with *Halomonas campisalis*: kinetics of dentrification at pH 9 and 12.5% NaCl. *Water Res.* , **35** (17), 4237-42.

Rittmann, B. E., Personal Communication, 2 February 2002.

Rittmann, B. E., and Huck, P. M. (1989) Biological treatment of public water supplies. *CRC Critical Reviews on Environmental Engineering Control*, 1**19**(2), 119-184.

Rittmann, B. E., and Snoeyink, V. L. (1984) Achieving biologically stable drinking water. *Journal AWWA*, **76**(10), 106.

Sakakibara, Y., and Kusaka, J. (1999) In situ autotrophic denitrification using electrode under oligotrophic conditions. *Int. In Situ On-Site Biorem. Symp., 5th*, 4 73-78. Publisher: Battelle Press, Columbus, Ohio

Schultz, K. L. (1960) Load and efficiency of trickling filters, *Journal WPCF*, **33**(3), 245-260.

Schwarz, S. E.; Semmens, M. J.; and Froelich, K. J. (1991) Membrane Air-Stripping: Operating Problems and Cost Analysis, *45th Purdue Indust. Waste Conf. Proc.*, 547-556.

Sell, M.; Ross, B. ; Feist, H.; Behling, R.; Kneifel, K.; and Peinemann, K.V (1993) Hydrogen transport into water via hollow fiber membranes for catalytic nitrate removal. *Proceedings – Membrane Technology Conference*, American Water Works Assoc., Denver, Colo, pp. 471-90.

Semmens, M. J. (1991) Bubbleless gas transfer device and process, *US Patent # 5,034,164.*

Shuvai, H. I., and Gruener, V. (1977) Infant Methomoglobinemia and other health effects of nitrates in drinking water. *Prog. Water Tech,.* **8**(4-5),183.

Smith, R.L., Ceazan, M.L. and Brooks, M.H. (1994) Autotrophic, Hydrogen Oxidizing, Denitrifying Bacteria in Groundwater, Potential Agents for Bioremediation of Nitrate Contamination, *Appl. Environ. Microbiol.*, **60**(6), 1949-1955.

Szekeres, S.; Kiss, I.; Bejerano, T.; and Soarez, M.I. (2001) Hydrogen-dependent denitrification in a two-reactor bio-electrochemical system. *Water Res.*, **35**(3), 715-719.

Tadashi, M., and Kato. T. (2001) Removal of nitrogen from wastewater with autotrophic bacteria. *Jpn. Kokai Tokkyo Koho*. pp.7.

Till, B. A.; Weathers, L. J.; and Alvarez, P. J. (1997) Treatment of nitrate-contaminated waters using autotrophic denitrifiers and Fe(O). *Proc. Water Environ. Fed. 70th Annu. Tech. Exposition Conf.*, 237-243.

Till, B. A.; Weathers, L. J.; and Alvarez, P. J. (1998) Fe(O)-supported autotrophic denitrification. *Environ.l Sci. Technol.*, **32**(5), 634-639.

Uemoto, H., and Saiki, H. (2000) Distribution of *Nitrosomonas europaea* and *Paracoccus denitrificans* immobilized in tubular polymeric gel for nitrogen removal. *Appl. Environ.l Microbiol.*, **66**(2), 816-819.

Urbain, V.; Benoid, R.; and J. Manem (1996) Membrane bioreactor: a new treatment tool. *J. - Am. Water Works Assoc.*, **88**,75-86.

USEPA (1993) *Manual for nitrogen control.* U.S.Environmental Protection Agency Technical Report, EPA/625/R-93/010, Office of Research and Development and Office of Water, Washington, DC.

USEPA (1998) *Technical Protocol for Evaluating Natural Attenuation of Chlorinated Solvents in Groundwater*, EPA/600/R-98/128, Office of Research and Development and Office of Water, Washington, DC.

van der Hoek, J. P.; van der Hoek, W. F; and Klapwijk, A. (1988) Nitrate removal from groundwater – use of a nitrate selective resin and a low concentrated regenerant, *Water, Air and Soil Pollution.*, **37**,41.

van Houten, R.; Hulshoff Pol, L.W.; and Lettinga, G. (1994) Biological Sulfate Reduction Using Gas-Lift Reactors Fed with Hydrogen and carbon Dioxide as Energy and Carbon Source, *Biotechnol. Bioeng.*, **44**, 586-594.

Viraraghavan, T., and Rao, G. A. K. (1990) Treatment processes nitrate removal from water, *Proc. 42nd Annu. Convention of Western Canada Water and Wastewater Assn.*, Regina, Sask., Can, 137-160.

Weber, W.J., and DiGiano, F. A, (1996) *Process Dynamics in Environmental Systems*, John Wiley and Sons, New York.

Yang, M. C., and Cussler, E.L. (1986) Designing hollow fiber contactors, *AIChE Journal*, **32**(11), 1910-1916.

# APPENDIX A

## Batch Reactor Data for Carbon Dioxide as Carbon Source

### Nitrate-Nitrogen Concentration

| Time (hours) | Reactor #1 (mg /L) | Reactor #2 (mg /L) | Reactor #3 (mg /L) | Reactor #4 (mg /L) | Control (mg /L) |
|---|---|---|---|---|---|
| 0 | 23.101 | 23.101 | 23.346 | 23.346 | 24.980 |
| 22 | 24.392 | 23.169 | 23.067 | 24.800 | 24.902 |
| 42.5 | 7.168 | 0.849 | 3.295 | 4.230 | 24.500 |
| 66 | 4.552 | 2.065 | 0.883 | 1.290 | 24.500 |
| 90.25 | 2.736 | 0.222 | 0.782 | 0.560 | 23.980 |
| 113.25 | 1.266 | 0.060 | 0.568 | 0.450 | 24.500 |
| 142 | 0.101 | 0.361 | 0.247 | 0.321 | 24.780 |
| 161 | 0.272 | 0.264 | 0.133 | 0.068 | 23.900 |
| 185.5 | 0.076 | 0.133 | 0.133 | 0.117 | 24.130 |

### Nitrite-Nitrogen Concentration

| Time (hours) | Reactor #1 (mg /L) | Reactor #2 (mg /L) | Reactor #3 (mg /L) | Reactor #4 (mg/L) | Control (mg /L) |
|---|---|---|---|---|---|
| 0 | 0.0 | 0.0 | 0.0 | 0.0 | 0 |
| 22 | 2.3 | 4.3 | 3.4 | 3.4 | 0 |
| 42.5 | 6.9 | 10.3 | 6.9 | 7.6 | 0 |
| 66 | 10.3 | 7.9 | 10.3 | 5.2 | 0 |
| 90.25 | 3.4 | 3.4 | 10.3 | 4.4 | 0 |
| 113.25 | 2.1 | 3.4 | 4.8 | 3.4 | 0 |
| 142 | 2.7 | 3.4 | 2.7 | 2.1 | 0 |
| 161 | 1.4 | 1.4 | 1.4 | 2.1 | 0 |
| 185.5 | 0.7 | 1.0 | 0.7 | 1.4 | 0 |

## Protein Concentration

| Time (hours) | Reactor #1 (mg /L) | Reactor #2 (mg /L) | Reactor #3 (mg /L) | Reactor #4 (mg/L) | Control (mg /L) |
|---|---|---|---|---|---|
| 0 | 5.48 | 4.56 | 5.1 | 4.80 | 0 |
| 22 | 5.51 | 5.13 | 5.78 | 6.23 | 0 |
| 42.5 | 7.89 | 8.60 | 8.2 | 7.50 | 0 |
| 66 | 9.04 | 11.23 | 12.54 | 8.40 | 0 |
| 90.25 | 14.89 | 12.76 | 15.2 | 14.65 | 0 |
| 113.25 | 15.21 | 14.02 | 16.12 | 14.02 | 0 |
| 142 | 18.84 | 17.89 | 18.12 | 18.85 | 0 |
| 161 | 15.12 | 14.56 | 14.67 | 16.56 | 0 |
| 185.5 | 14.8 | 14.20 | 13.89 | 16.10 | 0 |

## Average pH and Alkalinity

| Time (hours) | Average pH | Average Alkalinity (mg/L as $CaCO_3$) |
|---|---|---|
| 0 | 7.42 | 400 |
| 22 | 7.33 | 410 |
| 42.5 | 7.20 | 413 |
| 66 | 6.95 | 445 |
| 90.25 | 7.05 | 449 |
| 113.25 | 6.91 | 440 |
| 142 | 7.62 | 459 |
| 161 | 7.61 | 452 |
| 185.5 | 7.54 | 460 |

## Batch Reactor Data for Carbonate as Carbon Source

### Nitrate-Nitrogen Concentration

| Time (hours) | Reactor #1 (mg /L) | Reactor #2 (mg /L) | Reactor #3 (mg /L) | Reactor #4 (mg/L) | Control (mg /L) |
|---|---|---|---|---|---|
| 0.00 | 25.195 | 23.597 | 24.032 | 24.178 | 24.032 |
| 0.59 | 22.512 | 23.088 | 22.434 | 23.451 | 23.675 |
| 0.92 | 18.673 | 23.306 | 19.963 | 23.306 | 24.123 |
| 1.69 | 13.099 | 21.271 | 13.787 | 19.818 | 24.032 |
| 2.62 | 5.123 | 13.714 | 4.122 | 12.240 | 24.127 |
| 3.49 | 4.914 | 4.059 | 4.495 | 5.222 | 23.127 |
| 4.55 | 4.733 | 3.914 | 4.023 | 4.495 | 23.326 |
| 6.48 | 4.641 | 1.189 | 1.044 | 2.098 | 24.008 |
| 7.53 | 3.218 | 1.001 | 0.740 | 1.775 | 23.761 |
| 9.54 | 1.253 | 0.401 | 0.068 | 0.522 | 24.513 |

### Nitrite-Nitrogen Concentration

| Time (hours) | Reactor #1 (mg /L) | Reactor #2 (mg /L) | Reactor #3 (mg /L) | Reactor #4 (mg/L) | Control (mg /L) |
|---|---|---|---|---|---|
| 0.00 | 0.0 | 0.0 | 0.0 | 0.0 | 0 |
| 0.59 | 0.0 | 0.0 | 1.0 | 0.7 | 0 |
| 0.92 | 0.3 | 0.1 | 2.1 | 1.4 | 0 |
| 1.69 | 0.0 | 0.0 | 9.3 | 3.4 | 0 |
| 2.62 | 0.3 | 0.1 | 19.6 | 3.8 | 0 |
| 3.49 | 0.3 | 0.1 | 16.1 | 20.3 | 0 |
| 4.55 | 3.8 | 1.3 | 16.8 | 16.8 | 0 |
| 6.48 | 21.0 | 7.2 | 8.2 | 11.0 | 0 |
| 7.53 | 18.5 | 6.4 | 4.1 | 7.2 | 0 |
| 9.54 | 19.2 | 6.6 | 1.0 | 3.4 | 0 |

## Protein Concentration

| Time (hours) | Reactor #1 (mg /L) | Reactor #2 (mg /L) | Reactor #3 (mg /L) | Reactor #4 (mg/L) | Control (mg /L) |
|---|---|---|---|---|---|
| 0 | 1.6 | 2 | 1.5 | 1.7 | 0 |
| 59.24 | 12 | 12 | 12 | 10 | 0 |
| 230 | 15 | 16 | 19 | 20 | 0 |

## Average pH and Alkalinity

| Time (hours) | Average pH | Average Alkalinity (mg/L as $CaCO_3$) |
|---|---|---|
| 0 | 6.2 | 400 |
| 14.25 | 6.4 | 424 |
| 22 | 6.3 | 438 |
| 40.49 | 6.5 | 450 |
| 62.99 | 6.5 | 450 |
| 83.74 | 6.6 | 448 |
| 109.24 | 6.8 | 447 |
| 155.49 | 6.9 | 445 |
| 180.74 | 6.8 | 450 |
| 228.99 | 7 | 448 |

# APPENDIX B

## Table B1: Parameters for the Sealed-end Hollow Fiber Experiments

| Pressure (psig) | Water velocity (cm/s) | kL (cm/s) | ln(v) | ln(kL) |
|---|---|---|---|---|
| 1 | 14.08 | 0.000116 | 2.645 | -9.07 |
| 1 | 22.98 | 0.000231 | 3.135 | -8.37 |
| 1 | 30.79 | 0.000981 | 3.427 | -6.93 |
| 1 | 38.16 | 0.001059 | 3.642 | -6.85 |
| 2 | 14.08 | 0.000288 | 2.645 | -8.15 |
| 2 | 22.98 | 0.001065 | 3.135 | -6.84 |
| 2 | 30.79 | 0.001451 | 3.427 | -6.54 |
| 2 | 38.16 | 0.001322 | 3.642 | -6.63 |
| 3 | 14.08 | 0.000707 | 2.645 | -7.25 |
| 3 | 22.98 | 0.001562 | 3.135 | -6.46 |
| 3 | 30.79 | 0.002357 | 3.427 | -6.05 |
| 3 | 38.16 | 0.002100 | 3.642 | -6.17 |
| 4 | 14.08 | 0.001303 | 2.645 | -6.64 |
| 4 | 22.98 | 0.002662 | 3.135 | -5.93 |
| 4 | 30.79 | 0.002667 | 3.427 | -5.93 |
| 4 | 38.16 | 0.002820 | 3.642 | -5.87 |

**Table B2: Parameters for the Flow-through Hollow Fiber Modules**

| Run # | No. of Fibers | Diameter of fiber (cm) | Length of fiber (cm) | Diameter of shell (cm) | Velocity (cm/s) |
|---|---|---|---|---|---|
| 1 | 36 | 0.03 | 129 | 0.6 | 62.84 |
| 2 | 36 | 0.03 | 129 | 0.6 | 58.24 |
| 3 | 36 | 0.03 | 129 | 0.6 | 51.03 |
| 4 | 36 | 0.03 | 129 | 0.6 | 43.82 |
| 5 | 36 | 0.03 | 129 | 0.6 | 36.61 |
| 6 | 36 | 0.03 | 129 | 0.6 | 29.40 |
| 7 | 36 | 0.03 | 129 | 0.6 | 22.19 |
| 8 | 36 | 0.03 | 129 | 0.6 | 14.98 |
| 9 | 36 | 0.03 | 129 | 0.6 | 7.773 |
| 10 | 6 | 0.03 | 69 | 0.6 | 114.3 |
| 11 | 6 | 0.03 | 69 | 0.6 | 90.36 |
| 12 | 6 | 0.03 | 69 | 0.6 | 65.45 |
| 13 | 6 | 0.03 | 69 | 0.6 | 60.47 |
| 14 | 6 | 0.03 | 69 | 0.6 | 53.81 |
| 15 | 6 | 0.03 | 69 | 0.6 | 47.15 |
| 16 | 6 | 0.03 | 69 | 0.6 | 40.48 |
| 17 | 6 | 0.03 | 69 | 0.6 | 40.48 |
| 18 | 6 | 0.03 | 69 | 0.6 | 36.50 |
| 19 | 6 | 0.03 | 69 | 0.6 | 33.82 |
| 20 | 6 | 0.03 | 69 | 0.6 | 33.82 |
| 21 | 6 | 0.03 | 69 | 0.6 | 27.16 |
| 22 | 6 | 0.03 | 69 | 0.6 | 27.16 |
| 23 | 6 | 0.03 | 69 | 0.6 | 20.50 |
| 24 | 6 | 0.03 | 69 | 0.6 | 13.84 |
| 25 | 1 | 0.03 | 80 | 0.6 | 59.71 |
| 26 | 1 | 0.03 | 80 | 0.6 | 53.13 |
| 27 | 1 | 0.03 | 80 | 0.6 | 46.55 |
| 28 | 1 | 0.03 | 80 | 0.6 | 39.98 |
| 29 | 1 | 0.03 | 80 | 0.6 | 33.40 |
| 30 | 1 | 0.03 | 80 | 0.6 | 26.82 |
| 31 | 1 | 0.03 | 80 | 0.6 | 20.25 |
| 32 | 1 | 0.03 | 80 | 0.6 | 13.67 |
| 33 | 1 | 0.03 | 80 | 0.6 | 3.803 |
| 34 | 1 | 0.03 | 71 | 0.4 | 134.8 |
| 35 | 1 | 0.03 | 71 | 0.4 | 119.9 |
| 36 | 1 | 0.03 | 71 | 0.4 | 105.1 |
| 37 | 1 | 0.03 | 71 | 0.4 | 90.23 |
| 38 | 1 | 0.03 | 71 | 0.4 | 75.39 |
| 39 | 1 | 0.03 | 71 | 0.4 | 45.70 |
| 40 | 6 | 0.03 | 63.5 | 0.4 | 288.2 |
| 41 | 6 | 0.03 | 63.5 | 0.4 | 245.7 |
| 42 | 6 | 0.03 | 63.5 | 0.4 | 207.3 |
| 43 | 6 | 0.03 | 63.5 | 0.4 | 151.0 |
| 44 | 6 | 0.03 | 63.5 | 0.4 | 91.97 |

**Table B3: The Mass Transfer Coefficients and Dimensionless Numbers**

| Run # | $k_L$(cm/s) | Sh | Re | $Red_e/l$ |
|---|---|---|---|---|
| 1 | 0.00872 | 85.01 | 712.96 | 1.08 |
| 2 | 0.00711 | 69.34 | 634.43 | 0.96 |
| 3 | 0.00518 | 50.50 | 555.89 | 0.84 |
| 4 | 0.00534 | 52.04 | 477.35 | 0.72 |
| 5 | 0.00280 | 27.33 | 398.82 | 0.60 |
| 6 | 0.00182 | 17.77 | 320.28 | 0.48 |
| 7 | 0.00176 | 17.13 | 241.75 | 0.37 |
| 8 | 0.00127 | 12.36 | 163.21 | 0.25 |
| 9 | 0.00118 | 11.47 | 84.67 | 0.13 |
| 10 | 0.02694 | 612.39 | 2902.82 | 19.13 |
| 11 | 0.02289 | 520.42 | 2294.90 | 15.12 |
| 12 | 0.02243 | 509.95 | 1595.79 | 10.51 |
| 13 | 0.01721 | 391.13 | 1535.61 | 10.12 |
| 14 | 0.01596 | 362.72 | 1366.46 | 9.00 |
| 15 | 0.01682 | 382.34 | 1197.30 | 7.89 |
| 16 | 0.00933 | 212.19 | 1028.15 | 6.77 |
| 17 | 0.01441 | 327.45 | 1028.15 | 6.77 |
| 18 | 0.01910 | 434.12 | 927.08 | 6.11 |
| 19 | 0.01404 | 319.06 | 858.99 | 5.66 |
| 20 | 0.01294 | 294.15 | 858.99 | 5.66 |
| 21 | 0.01132 | 257.32 | 689.84 | 4.55 |
| 22 | 0.01445 | 328.37 | 689.84 | 4.55 |
| 23 | 0.01424 | 323.62 | 520.68 | 3.43 |
| 24 | 0.01383 | 314.45 | 351.53 | 2.32 |
| 25 | 0.08554 | 2437.88 | 1901.23 | 13.55 |
| 26 | 0.08043 | 2292.36 | 1691.80 | 12.05 |
| 27 | 0.07638 | 2176.97 | 1482.37 | 10.56 |
| 28 | 0.05558 | 1583.96 | 1272.94 | 9.07 |
| 29 | 0.04521 | 1288.53 | 1063.51 | 7.58 |
| 30 | 0.04214 | 1201.08 | 854.09 | 6.09 |
| 31 | 0.03986 | 1135.91 | 644.66 | 4.59 |
| 32 | 0.03697 | 1053.58 | 435.23 | 3.10 |
| 33 | 0.02938 | 837.31 | 121.08 | 0.86 |
| 34 | 0.11651 | 2155.53 | 2785.52 | 14.52 |
| 35 | 0.11367 | 2102.89 | 2478.69 | 12.92 |
| 36 | 0.09000 | 1664.91 | 2171.85 | 11.32 |
| 37 | 0.06218 | 1150.25 | 1865.01 | 9.72 |
| 38 | 0.05713 | 1056.85 | 1558.17 | 8.12 |
| 39 | 0.05391 | 997.38 | 944.50 | 4.92 |
| 40 | 0.04614 | 614.99 | 4292.13 | 18.02 |
| 41 | 0.03958 | 527.55 | 3658.53 | 15.36 |
| 42 | 0.03425 | 456.47 | 3086.25 | 12.96 |
| 43 | 0.02628 | 350.23 | 2248.26 | 9.44 |
| 44 | 0.02348 | 312.97 | 1369.40 | 5.75 |

# APPENDIX C

**Table C1: Continuous Flow Reactor System Operation Data**

| HRT (hours) | Time (hours) | Nitrate Concentration (mg $NO_3$-N /L) | Nitrite Concentration (mg $NO_2$-N /L) | Alkalinity (mg/L as $CaCO_3$) | pH |
|---|---|---|---|---|---|
| 10 | 24 | 6.45 | 2.75 | 380 | 6.68 |
| 10 | 45 | 0.50 | 2.75 | 590 | 6.57 |
| 10 | 71.5 | 0.10 | | | 5.85 |
| 10 | 94 | 0.14 | 0.69 | 656 | 6.52 |
| 10 | 118 | -0.64 | 6.18 | 628 | |
| 10 | 143 | -0.15 | 5.50 | 619 | 6.64 |
| 10 | 166 | -0.23 | 2.06 | 624 | |
| 10 | 176 | -0.23 | | 574 | |
| 10 | 189 | -0.23 | | 548 | |
| 10 | 213 | -0.35 | | 546 | |
| 10 | 238 | -0.35 | 2.06 | 530 | 6.54 |
| 10 | 285 | -0.39 | 1.37 | 556 | 6.65 |
| 10 | 310 | -0.43 | 1.72 | 540 | 6.47 |
| 6.75 | 24 | 15.34 | 1.37 | 488 | 7.26 |
| 6.75 | 53 | 0.91 | 1.37 | 534 | 7.26 |
| 6.75 | 103 | -0.07 | 0.69 | 580 | 7.31 |
| 6.75 | 125 | -0.48 | 0.69 | 580 | 7.29 |
| 6.75 | 148 | -0.92 | 0.69 | 578 | 7.31 |
| 6.75 | 177.5 | -0.72 | 0.69 | 574 | 7.3 |
| 6.75 | 196.5 | -0.84 | 0.69 | 568 | 7.3 |
| 6.75 | 219 | -0.80 | 0.69 | 572 | 7.27 |
| 6.75 | 244 | -0.96 | 0.69 | 560 | 7.28 |
| 6.75 | 295 | -0.27 | 0.69 | 528 | 7.24 |
| 6.75 | 302 | -0.31 | 0.34 | 532 | 7.26 |
| 6.75 | 313 | -0.27 | 1.03 | 528 | 7.19 |
| 3.25 | 325 | -0.43 | 0.69 | 540 | |
| 3.25 | 338 | -0.27 | 0.69 | | |
| 3.25 | 366 | -0.39 | 0.69 | | |
| 3.25 | 386 | -0.27 | 0.69 | 552 | |
| 1.75 | 396 | -0.92 | 0.69 | 512 | 7.24 |
| 1.75 | 415 | 2.46 | 0.69 | 548 | 7.3 |
| 1.75 | 439 | 1.48 | 0.69 | 556 | 7.37 |
| 1.75 | 465 | -0.07 | 0.69 | 528 | 7.3 |
| 1.75 | 485.5 | 1.36 | 0.69 | | |
| 1.75 | 508.5 | 1.20 | 0.69 | | |
| 1.75 | 514.5 | 1.28 | | | |